

QUANTUM DIFFUSION IN OPTICAL LATTICES

A Thesis

by

TAYLOR BAILEY

Submitted to the Office of Graduate Studies and Research
Texas A&M University-Commerce
In partial fulfillment of the requirements
for the degree of
MASTER OF SCIENCE
May 2012

QUANTUM DIFFUSION IN OPTICAL LATTICES

A Thesis

by

TAYLOR BAILEY

Approved by:

Advisor:

Carlos Bertulani

Committee:

Carlos Bertulani
Kent Montgomery
Bao-An Li

Head of Department:

Kent Montgomery

Dean of the College:

Grady Blount

Dean of Graduate Studies and Research:

Allan Headley

ABSTRACT

QUANTUM DIFFUSION IN OPTICAL LATTICES

Taylor Bailey, MS
Texas A&M University-Commerce, 2012

Advisor: Carlos Bertulani, PhD

While in the optical lattice, molecules and atoms arising from the dissociation of molecules experience a one-dimensional sinusoidal potential induced by focusing and interfering laser beams. The laser field is a superposition of incoming and reflected waves. The idea is that even though the composite objects are classically confined within certain regions in space, these objects are able to hop across the potential barriers. Thus, the physics of optical lattice tunneling of composite objects by molecules generated by the Feshbach resonance method is of large interest in atomic physics and basic quantum phenomena. (Donley et al., 2001; Feshbach, 1958; Lewenstein & Liu, 2011) The purpose of the study is to numerically obtain the wave function, as well as the bound state energy levels. I was able to solve the one-dimensional double hump barrier for a composite particle, still of discussion in the literature. The problem consists of a loosely-bound molecule trapped inside of a cavity. The molecule can tunnel through a one-dimensional barrier, described by a potential acting on each of its atoms, and is able to break apart during the tunneling process. (Bertulani et al., 2007) The actual calculations used to determine the molecules wave function is found by solving the Schrödinger equation by means of iterative techniques. Since the square of

the amplitude of the wave function represents a probability density, the wave function must then be normalized to be of any practical use for physical applications. The inevitable goal would be to solve for a three-dimensional optical lattice. Extending the double hump barrier will cause the potential to turn into a series of barriers in three dimensions; thus, becoming a three-dimensional optical lattice. In order to undertake this project, numerical calculations utilizing computer codes would need to be performed. In addition, the process of clarifying the physics contained in the numerical results, along with a review of consistency tests, and a comparison to previous calculations will need to be performed. The results will provide analytical insights of the diffusion time on the lattice parameters and are worth publishing in a scientific journal.

Acknowledgements

It is with deep and sincere appreciation that I recognize and commend Dr. Carlos Bertulani for challenging me to reach my fullest potential as a life-long learner and for teaching me life lessons that I will take with me as I begin my post-graduate journey. Not only am I perpetually grateful for Carlos's mentorship during my tenure at Texas A&M University-Commerce but for his enduring friendship. I am also beholden to Carlos for all of his assistance on my project, and for his patience, without which the development of my graduate project would not have been possible.

Furthermore, I would like to thank Arturo Samana for all his hard work and effort in early preliminary findings.

I am thankful to Dr. Charles Rogers who made the classroom learning come alive through hands-on problem based learning that sparked a renewed passion for ingenuity within in me.

I am also indebted to my friends and peers, Porntip "Tiffany" Leeprapaiwong in particular, not only for all of their unending support, encouragement, and camaraderie, but for sharing their perspectives on life and foundational concepts with me. My perception will forever be changed for the better because of their impact.

I would like to thank my parents and my grandmother for all they have done for me, for the encouragement they have given me throughout my educational career, as well as for the all of their financial support.

Lastly, I would like to thank the Physics Department for their financial support and for affording me the opportunity to be a teaching assistant. Correspondingly, I am also appreciatory to the National Science Foundation - STEM and Texas A&M University-Commerce Graduate School for their financial support.

Table of Contents

1	INTRODUCTION	1
2	QUANTUM TUNNELING	2
2.1	Time-dependent probabilities	2
2.2	Landau (or Oppenheimer) Approximation	4
2.3	The WBK-Landau-Oppenheimer approximation	8
2.4	Double-well with analytical solution	11
3	OPTICAL LATTICES	14
3.1	Introduction	14
3.2	The Lorentz Model	15
3.3	Optical Lattices	16
3.4	Application	18
4	FESHBACH MOLECULES	19
4.1	Scattering	19
4.1.1	Differential Cross Section	19
4.1.2	Partial waves	21
4.2	Feshbach Molecules	25
5	TUNNELING, DIFFUSION AND DISSOCIATION OF FESHBACH MOLECULES IN OPTICAL LATTICES	29
5.1	Introduction	29
A	THE ONE-DIMENSIONAL WKB APPROXIMATION	44
B	SCHRÖDINGER EQUATION IN A SPACE-TIME LATTICE	54

List of Figures

2.1	Schematic double-well potential.	6
2.2	Double square-well potential.	11
2.3	Energy dependence of the levels in the double square-well potential as a function of the width of the second well. The calculations are done by solving the transcendental equation (2.43).	12
3.1	One-Dimensional Optical Lattice	15
4.1	Due to the different magnetic moments the closed channel can be shifted relative to the open channel by applying a magnetic field. Tuning a bound state of the closed channel to degeneracy with the continuum of the open channel leads to a Feshbach resonance.	27
4.2	Due to the different magnetic moments the closed channel can be shifted relative to the open channel by applying a magnetic field. Tuning a bound state of the closed channel to degeneracy with the continuum of the open channel leads to a Feshbach resonance.	28
5.1	Time evolution of the probability distribution of strongly bound ($E_b = 10$ kHz) Rubidium molecules in an optical lattice with size $D = 2 \mu\text{m}$. From top to bottom the time is $t = 0$, $t = 10$ ms, $t = 25$ ms and $t = 100$ ms, respectively.	35
5.2	Time dependence of the escape probability of strongly bound Rubidium molecules from an optical lattice with size $D = 2 \mu\text{m}$, as a function of increasing potential barrier heights. The barrier height increases each time by a factor of 1.5 in going from the solid to dashed-dotted, from dashed-dotted to long-dashed, and from long-dashed to dotted curve.	36

5.3	Time dependence of the “integrity” probability of loosely bound Rubidium molecules by tunneling and diffusion through an optical lattice with lattice constant $D = 2 \mu\text{m}$, and potential barrier height $V_0=5 \text{ kHz}$. The integrity is the probability that the molecule remains in its bound state. The binding energies were parametrized in terms of the barrier height, with $E_4 = V_0/20$, $E_3 = V_0/5$, $E_2 = V_0/2$, and $E_1 = V_0/1.2$	38
5.4	Lattice diffusion of molecules. The hatched histograms are the relative probability of finding a molecule in its ground state at a given position along the lattice. The solid histograms give the relative probability of finding individual atoms after the dissociation. This figure was generated for the highest dissociation probability (20%) described in figure 5.3.	39
5.5	Time dependence of the spreading width of bound molecules, $\sigma_M(t)$, shown in solid line and of dissociated atoms, $\sigma_A(t)$, shown in dotted line, defined in the text. The dashed curve is a fit of the asymptotic time-dependence with the analytical formula, Eq. (5.15).	40
A.1	Classically forbidden (I) and classically allowed (II) regions.	48
A.2	Integration path in the complex plane for the connection formulas.	50

Chapter 1

INTRODUCTION

The birth of quantum mechanics stems from the limitations of classical mechanics - as the study of particles bound by classical theory does not explain phenomena observed at the turn of the 20th century. One such example would be in the explanation of alpha decay, whereby the nucleus of an unstable atom emits an alpha particle. From classical mechanics, an incoming object can react to a potential barrier in one of two ways: the object may undergo full transmission, whereby the object fully overcomes the barrier, or it may undergo full reflection, whereby the object completely rebounds from the barrier - all depending on the kinetic energy of the incoming object. As early experiments showed, even if an object does not have the required energy to classically overcome a barrier, it still possesses the ability to penetrate it. Coming back to our example of alpha decay, even though the nuclear force inside the nucleus of an atom is much stronger than the repulsive electrostatic force exerted by all the positively charged protons, we observe the emission of a helium nucleus, known as an alpha particle. This phenomenon was first explained in 1928 by George Gamow via quantum tunneling.

Quantum tunneling is at the heart of this research, as we study the diffusion of atoms and molecules through periodic potential landscapes. In the upcoming chapters, I would like to discuss how such artificial barriers are created, as well as the method of taking two unbound atoms and forming a single molecule from them. By first explaining the basics, I hope to give the reader a foundation that will allow him/her to follow along for when I start discussing the research that has been done, as well as, to give the reader a sample of what has been accomplished in the field of cold atom physics. Also, I would like to answer such questions as: what are the tunneling times of the molecules inside the periodic potential barriers versus the individual particles that make them up, whether tunneling favors molecules or the dissociation of those molecules - as we adjust the lattice parameters and the interaction between atoms making up the molecules?

Chapter 2

QUANTUM TUNNELING

Tunneling is a phenomena observed only for quantum systems. I would like consider the following problem to illustrate the idea. Suppose we have an incoming particle, such as an electron, approaching a potential barrier centered at the origin. For simplicity, our potential is a finite square barrier that is everywhere zero, except at the barrier. If a classical particle approaches such a barrier, one of two outcomes will occur: the particle will overcome the barrier-resulting in full transmission-or the particle will rebound off the barrier-resulting in full reflection. The outcome hinges on whether the kinetic energy of the particle's is greater than the potential barrier. When we consider a quantum particle, quantum theory allows for the partial transmission and reflection of the particle, assuming the barrier has finite width and height. This is in sharp contrast with classical theory, because even if the particle's energy is less than the potential barrier, it is still possible for the particle to penetrate the barrier. This is known as quantum tunneling.

2.1 Time-dependent probabilities

The Hamiltonian for a one-dimensional system is

$$\mathcal{H} = \frac{\hat{p}^2}{2m} + V(x). \quad (2.1)$$

The potential $V(x)$ of interest will be in the form of a double well. We are also interested in confining potentials. Thus, we will be dealing with a discrete spectrum, having a set of eigenfunctions $|\psi_n\rangle$ for the eigenvalue problem

$$\mathcal{H}|\psi_n\rangle = E_n|\psi_n\rangle, \quad (2.2)$$

where E_n are the corresponding eigen-energies.

The time-dependent wave function can be written as a linear combination

$$|\Psi(x, t)\rangle = \sum_n a_n |\psi_n(x, t)\rangle = \sum_n a_n e^{-iE_n t/\hbar} |\psi_n(x, 0)\rangle, \quad (2.3)$$

in terms of the stationary states $|\psi(x, 0)\rangle \equiv |\psi_n\rangle$. The solutions $|\psi_n\rangle$ of the time-independent problem are found by solving equation (2.1); therefore, the basis may be written as

$$|\psi_n(x, t)\rangle = e^{-iE_n t/\hbar} |\psi_n\rangle. \quad (2.4)$$

The time-dependent wave function $|\Psi(x, t)\rangle$ at $t = 0$ may be expressed as

$$|\Psi(x, 0)\rangle = \sum_n a_n |\psi_n\rangle \equiv |\Psi_0\rangle, \quad (2.5)$$

where the coefficients a_n in equation (2.5) are

$$a_n = \langle \psi_n | \Psi_0 \rangle = \int \psi_n^* \Psi_0 \, d\tau, \quad (d\tau = d^3r). \quad (2.6)$$

The basis wave functions $|\psi_n\rangle$ are orthonormalized

$$\langle \psi_m | \psi_n \rangle = \int \psi_m^* \psi_n \, d\tau = \delta_{m,n}. \quad (2.7)$$

and are solutions of the time-dependent Schrödinger equation

$$i\hbar \frac{\partial}{\partial t} |\psi_n(x, t)\rangle = E_n |\psi_n(x, t)\rangle. \quad (2.8)$$

The probability that at some time the system is localized within a region D is given by

$$P(t) = \langle \Psi(x, t) | \Psi(x, t) \rangle = \int_{(D)} \Psi^*(x, t) \Psi(x, t) \, d\tau. \quad (2.9)$$

Using the wavefunction $|\Psi(t)\rangle$ from (2.3), the probability is

$$P(t) = \sum_{n,m} e^{-i(E_n - E_m)t/\hbar} a_m^* a_n \int_{(D)} \psi_m^* \psi_n \, d\tau. \quad (2.10)$$

In assuming that the ψ_n are real, the probability $P(t)$ reads ¹

$$P(t) = P(t=0) - 4 \sum_{n,m>n} A_{n,m} \sin^2 \left(\frac{(E_n - E_m)t}{2\hbar} \right), \quad (2.11)$$

where

$$A_{m,n} = a_n a_m \int_{(D)} \psi_n \psi_m d\tau. \quad (2.12)$$

If Ψ_0 describes a particle localized within one of the two wells (say, well I) and if D represents the second well (D = well II), eqs. (2.11,2.12) determine the probability that the particle tunnels from well I to well II. It is important to notice that this probability depends essentially on the A_{nm} coefficients, which contains the spatial dependence of the localized wavefunctions.

As shown in the next section, the spatial distribution of the wavefunctions might generate resonant effects. The tunneling probability from well I to well II will be larger when the coefficients A_{nm} are correspondingly large. Therefore, two conditions must be satisfied.

- the Hamiltonian must allow at least two wavefunctions, ψ_n and ψ_m , that have an appreciable part within the well II. This condition allows that the term $\int_{(II)} \psi_n \psi_m d\tau$ be non-negligible.

- The eigenstates ψ_n and ψ_m must be the main components of Ψ_0 : thus, the coefficients a_n and a_m (and consequently A_{nm}) must be large enough.

As Ψ_0 is localized in well I, the second condition is not satisfied. Therefore, we conclude that Ψ must be composed by at least two states m and n whose spatial distributions are approximately equal.

2.2 Landau (or Oppenheimer) Approximation

We will now describe the Landau (or Oppenheimer) approximation. It is well described in (Landau & Lifshits, 1958). However it only discusses the case of a symmetric double well. We will be more general here. Let us assume that solutions exist for the

¹In the appendix is the proof of this step using the δ -function.

time-independent SE for both potential wells. We label the left well as (*I*)

$$-\frac{\hbar^2}{2m} \frac{d^2 \psi_n^I}{dx^2} + V(x) \psi_n^I = E_n^I \psi_n^I, \quad (2.13)$$

and the right well as (*II*)

$$-\frac{\hbar^2}{2m} \frac{d^2 \psi_m^{II}}{dx^2} + V(x) \psi_m^{II} = E_m^{II} \psi_m^{II}, \quad (2.14)$$

satisfying the orthogonality properties

$$\int_{-\infty}^{x_m} |\psi_n^I|^2 dx = \int_{x_m}^{\infty} |\psi_m^{II}|^2 dx = 1,$$

and

$$\int_{-\infty}^{\infty} \psi_n^I \psi_m^{II} dx = 0. \quad (2.15)$$

The last condition obviously implies that there is no tunneling between these two states (due to eq. 2.12). However, it allows us to build a simple method applied to cases in which tunneling is small.

Consider the point x_m as the middle of the potential barrier, with a height of V_m . The potential $V(x)$ can be decomposed as

$$V(x) = V^I(x) + V^{II}(x) - V_m \quad (2.16)$$

where

$$V^I(x) = \begin{cases} V(x) & , \quad \text{if } x < x_m, \\ V_m & , \quad \text{if } x \geq x_m, \end{cases} \quad (2.17)$$

$$V^{II}(x) = \begin{cases} V_m & , \quad \text{if } x < x_m, \\ V(x) & , \quad \text{if } x \geq x_m. \end{cases} \quad (2.18)$$

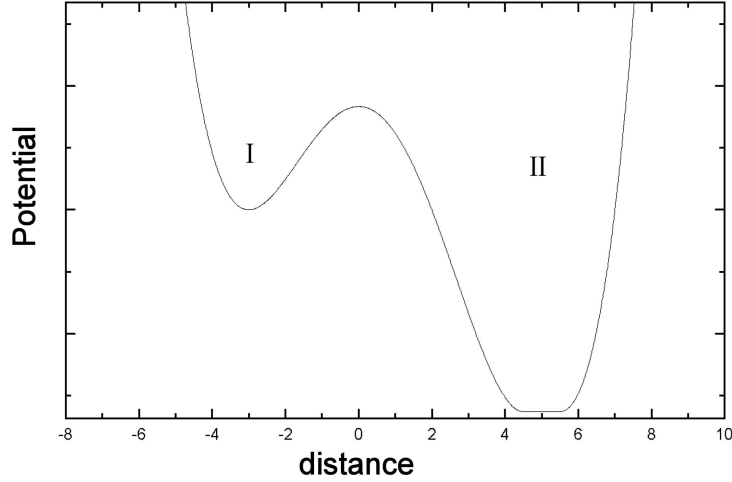


Figure 2.1: Schematic double-well potential.

The Landau approximation consists in building two eigen-states of \mathcal{H} from the states I and II, which have very close energies,

$$|E_n^I - E_m^{II}| \ll |E_n^I - E_j^{II}|, \quad \forall j \neq m. \quad (2.19)$$

This procedure allows the description of tunneling effects because a state build in this way would be localized at the same time in both wells I and II. For a double well, we can try a linear combination of the two isolated solutions in wells I and II, *i.e.*,

$$|\psi\rangle = \frac{|\psi_n^I\rangle + c|\psi_m^{II}\rangle}{\sqrt{1+c^2}} \quad (2.20)$$

where the factor $(1+c^2)^{-1/2}$ ensures that $\langle\psi|\psi\rangle = 1$. Now, the wave function $|\psi\rangle$ satisfies the SE

$$\left(-\frac{\hbar^2}{2m} \frac{d^2}{dx^2} + V(x)\right) |\psi\rangle = E|\psi\rangle. \quad (2.21)$$

Substituting the solution (2.20) into the Schrödinger equation (2.21), yields a quadratic equation of the coefficient c :

$$Qc^2 - \frac{2m}{\hbar}(E_m^{II} - E_n^I)c - Q = 0, \quad (2.22)$$

Where

$$Q = \frac{d\psi_n^I}{dx}(x_m)\psi_m^{II}(x_m) - \psi_n^I(x_m)\frac{d\psi_m^{II}}{dx}(x_m). \quad (2.23)$$

Q has the meaning of the current density at the point x_m .

We can prove the result above by multiplying equation (2.13) by ψ and then subtracting this result from the product of (2.21) with ψ_n^I . We obtain the integrand

$$\int_{-\infty}^{x_m} \left(\psi \frac{d^2\psi_n^I}{dx^2} - \psi_n^I \frac{d^2\psi}{dx^2} \right) d\tau = \frac{2m}{\hbar^2} (E - E_n^I) \int_{-\infty}^{x_m} \psi \psi_n^I d\tau \quad (2.24)$$

By integrating the right side of equation (2.24) and using the orthogonality condition

$$\int \psi_n^I \psi_m^{II} d\tau = 0, \quad (2.25)$$

along with integrating the left side of the equation and using the definition of Q , we obtain

$$\frac{2m}{\hbar^2} (E - E_n^I) = Qc. \quad (2.26)$$

A similar procedure with ψ and ψ_m^{II} using equations (2.14) and (2.21) will result in the following equation

$$\frac{2m}{\hbar^2} (E - E_m^{II}) = \frac{Q}{c}. \quad (2.27)$$

Form these two equations we can show that eq. 2.22 is right, as desired.

These conditions yield two roots for the quadratic equation of c (2.22) (*i.e.*, c_+ and c_-). We thus have two solutions for the wavefunction (2.20): ψ_+ and ψ_- , with energies E_+ and E_- respectively. From eq. 2.22, the coefficients c_{\pm} are

$$c_{\pm} = \frac{m}{\hbar^2 Q} \Delta E \pm \sqrt{1 + \left(\frac{m \Delta E}{\hbar^2 Q} \right)^2}, \quad (2.28)$$

where

$$\Delta E = E_m^{II} - E_n^I. \quad (2.29)$$

The wavefunctions (2.20) for the double-well potential are approximately given by

$$|\psi_{\pm}\rangle = \frac{1}{\sqrt{1+c_{\pm}^2}}|\psi_n^I\rangle + \frac{c_{\pm}}{\sqrt{1+c_{\pm}^2}}|\psi_m^{II}\rangle. \quad (2.30)$$

We can invert these solutions. For region (I), the wave function is

$$|\psi_n^I\rangle = -\frac{c_-}{c_+ - c_-}\sqrt{1+c_+^2}|\psi_+\rangle + \frac{c_+}{c_+ - c_-}\sqrt{1+c_-^2}|\psi_-\rangle, \quad (2.31)$$

and for region (II)

$$|\psi_m^{II}\rangle = \frac{1}{c_+ - c_-}\sqrt{1+c_+^2}|\psi_+\rangle - \frac{1}{c_+ - c_-}\sqrt{1+c_-^2}|\psi_-\rangle. \quad (2.32)$$

The energies for the double-well potential also depend on Q ,

$$E_{\pm} = E_n^I + \frac{\hbar^2}{2m}Qc_{\pm}. \quad (2.33)$$

According to these results, the energy between E_+ and E_- ,

$$\Delta\mathcal{E} = E_+ - E_- = \sqrt{(\Delta E)^2 + \left(\frac{\hbar^2 Q}{m}\right)^2}, \quad (2.34)$$

is of crucial relevance for the tunneling problem. Note that $\Delta\mathcal{E} > \Delta E$.

2.3 The WBK-Landau-Oppenheimer approximation

An easy way to calculate the quantities Q and $\Delta\mathcal{E}$ is to use the WKB approximation, which we summarize in appendix A. Using the WKB wavefunction in eq. 2.23 we get for

$\Delta\mathcal{E}$ the following expression:

$$\begin{aligned} \Delta\mathcal{E} = & \left\{ (\Delta E)^2 + \left[\hbar(v_1 + v_2) \sqrt{\frac{\omega_1}{2\pi v_1}} \sqrt{\frac{\omega_2}{2\pi v_2}} \right. \right. \\ & \times \exp \left(- \int_{a_1}^{x_M} \sqrt{\frac{2m}{\hbar}} (V(x) - E_n^I) dx \right. \\ & \left. \left. - \int_{x_M}^{a_2} \sqrt{\frac{2m}{\hbar}} (V(x) - E_m^{II}) dx \right) \right]^2 \Big\}^{1/2}. \end{aligned} \quad (2.35)$$

The classical oscillation frequencies for a particle with energy E_I in well I and energy E_{II} in well II are given by

$$\begin{aligned} \omega_1 &= \pi / \int_{b_1}^{a_1} \left[\frac{2}{m} (E_n^I - V(x)) \right]^{-1/2} dx \\ \omega_2 &= \pi / \int_{a_2}^{b_2} \left[\frac{2}{m} (E_m^{II} - V(x)) \right]^{-1/2} dx. \end{aligned} \quad (2.36)$$

And the coefficients are

$$\begin{aligned} v_1 &= \sqrt{\frac{2}{m} (V_M - E_n^I)} \\ v_2 &= \sqrt{\frac{2}{m} (V_M - E_m^{II})}. \end{aligned} \quad (2.37)$$

The parameters b_i and a_i are the classical turning points associated with the energy E_i in well (i).

If we consider that at $t = 0$ the particle is in state $\langle \psi_n^I |$ (wavefunction localized in well I) we can calculate the probability of barrier penetrability to the localized state $\langle \psi_m^I |$ in well II by

$$\rho_{I \rightarrow II} = |\langle \psi_m^{II} | e^{-iHt/\hbar} | \psi_n^I \rangle|^2 = (\rho_{I \rightarrow II})_{max} \sin^2 \frac{\Delta\mathcal{E}}{2\hbar} t, \quad (2.38)$$

where

$$(\rho_{I \rightarrow II})_{max} = \left[1 + \left(\frac{m\Delta E}{\hbar^2 Q} \right)^2 \right]^{-1}. \quad (2.39)$$

This method allows us to calculate three essential quantities.

- Resonances:

An important phenomenon occurs when $\Delta E = 0$: *resonant tunneling*. Eq. 2.39 shows that when this happens the tunneling probability is equal to 1. The resonance occurs because in the absence of tunneling the energy levels E_I and E_{II} are degenerate. The presence of tunneling raises this degeneracy. The energy difference in the presence of a resonance is (with $E_n^I = E_m^{II}$ and $v_1 = v_2$)

$$(\Delta\mathcal{E})_{res} = \frac{\sqrt{(\hbar\omega_1)(\hbar\omega_2)}}{\pi} \exp\left(-\int_{a_1}^{a_2} \sqrt{\frac{2m}{\hbar^2}(V(x) - E_n^I)} dx\right). \quad (2.40)$$

In the symmetric double-well case the frequencies ω_1 and ω_2 are equal and we obtain the Landau formula (Landau & Lifshits, 1958). On the other hand, eq. 2.40 shows that when $E_n^I = E_m^{II}$ the energy difference $\Delta\mathcal{E}$ is larger. Note that the coefficients c_+ and c_- become, respectively, $+1$ and -1 . This means that the wavefunctions ψ_+ and ψ_- are equally distributed between wells I and II.

- Tunneling times:

Eq. 2.38 shows that when the particle is in resonance, its position will oscillate between the wells with a frequency

$$\begin{aligned} \omega_{I \rightarrow II} &= \frac{(\Delta\epsilon)_{res}}{2\hbar} \\ &= \frac{\sqrt{\omega_1\omega_2}}{2\pi} \exp\left(-\int_{a_1}^{a_2} \sqrt{\frac{2m}{\hbar^2}(V(x) - E_n^I)} dx\right). \end{aligned}$$

To this frequency we can associate a time, t_{max} , for which $\rho_{II} = \rho_{II}^{max}$ (this is the tunneling time it takes for the particle in going from well I to well II), *i.e.*,

$$t_{max} = \frac{\hbar\pi}{(\Delta\mathcal{E})_{res}}. \quad (2.41)$$

Thus the energy difference $\Delta\mathcal{E}$ will determine the tunneling time.

- Coherence of a wavepacket:

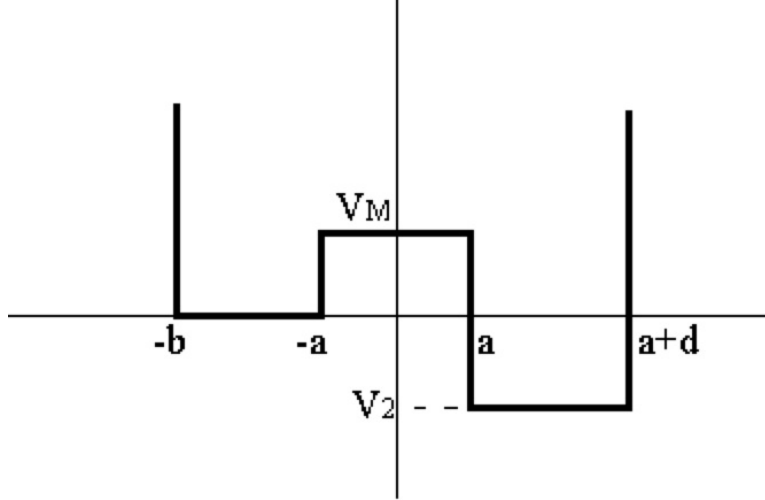


Figure 2.2: Double square-well potential.

We also see from these results that a wavefunction might not keep its form as it tunnels from one well to the other: a wavefunction with n nodes can become another one with m nodes ($n \neq m$) as it tunnels between the wells.

2.4 Double-well with analytical solution

Let us consider a double-well of the following form:

$$V(x) = \begin{cases} +\infty & \text{if } x < -b, \\ 0 & \text{if } -b \leq x < -a, \\ V_M & \text{if } -a \leq x < a, \\ V_2 & \text{if } a \leq x < a+d, \\ +\infty & \text{if } a+d \leq x. \end{cases} \quad (2.42)$$

We will consider $V_1 = 0$, $b - a = 3$ in appropriate units. Later, we will change the parameters associated with the well II (V_2, d) and with the barrier ($V_M, 2a$).

The eigen-energies ϵ (in the interval $[0, V_M]$) are obtained from the solution of the transcendental equations

$$\begin{aligned} \frac{k}{\gamma} \tanh 2\gamma a + \tan k(b-a) + \frac{k}{q} \tan qd \\ + \frac{\gamma}{q} \tan k(b-a) \tan qd \tanh 2\gamma a = 0, \end{aligned} \quad (2.43)$$

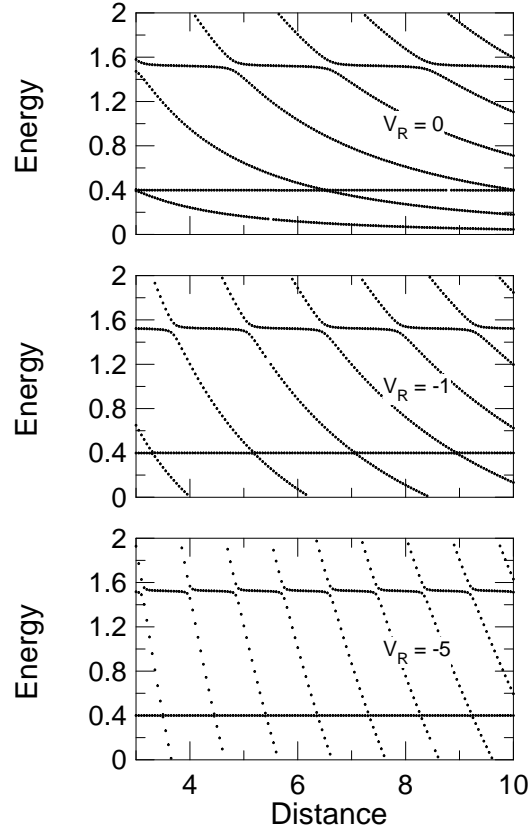


Figure 2.3: Energy dependence of the levels in the double square-well potential as a function of the width of the second well. The calculations are done by solving the transcendental equation (2.43).

where

$$k = \sqrt{2\epsilon}, \quad \gamma = \sqrt{2(V_M - \epsilon)}, \quad q = \sqrt{2(\epsilon - V_2)}. \quad (2.44)$$

To observe the characteristics of the potential in the energy spectrum, we will solve eq. (2.43) for different parameters of the potential. These results will be compared with the ones obtained with the decomposition of the potential in two separated wells, (V^I and V^{II}), Eq. (2.16).

The vertical scale of figure 2.3 represents the energies obtained with the exact solution for the potential (2.2), as a function of the width of the second well, for three values of V_2

($V_2 = 0$, $V_2 = -1$ and $V_2 = -5$). For all these values the barrier parameters are the same ($2a = 2$, $V_M = 2$). The two nearly visible horizontal lines correspond to the energies E_0^I and E_1^I of the potential V^I . These energies are obviously independent of d .

We clearly observe the resonant phenomena. The two energy levels of the left well remain nearly undisturbed due to the presence of the second well. But the second well influences the energy solution so that other levels appear. As d increases, the position of these additional levels change and their values come close together with those of the levels in the first well. When this happens, there is a “level repulsion” (or “non-level crossing”). The energy levels of the first well start to change, whereas the merging level takes over the nearly stable value of the eigen-energy of first well. This level repulsion is one of the most interesting results of quantum mechanics, appearing in numerous problems in physics. For certain values of d , there are two levels of energy E_m^{II} of the second well that are degenerate with the levels E_0^I and E_1^I of the first well. The same resonance phenomenon appears again for these values. As we will see later, the Landau approximation is also able to reproduce the same results.

Two other aspects are visible from this figure.

- a) The larger the depth V_2 of well I, the larger the number of values of d that generate the resonance. This is because, as V_2 increases, more bound states will be available in the second well and more possibilities for non-level crossing (resonance) occurs.
- b) The first excited level of the first well has its degeneracy removed in a more efficient way than that of the ground state. That is, the energy splitting is smaller for the ground state.

These resonant effects are equally visible if we analyze the tunneling probability to the second well, $(\rho_{I \rightarrow II})_{max}$, when the initial wavefunction corresponds to the ground state of the well I: $|\Psi\rangle = |\phi_n^I\rangle$. The calculation of $|\Psi\rangle = |\phi_n^I\rangle$ is done by means of an expansion of $|\phi_n^I\rangle$ in eigenstates of V of eq. (2.21). The next figure shows $(\rho_{I \rightarrow II})_{max}$ as a function of the width d of the second well.

Chapter 3

OPTICAL LATTICES

3.1 Introduction

An optical lattice is a tool which gives experimentalists control over individual atoms and molecules. The term lattice comes from the localization of the atoms or molecules in the pockets - occurring at equally spaced sites - of the potential landscape set up by the optical lattice. The lattice consists of interfering laser beams that create periodic regions of potential minima and maxima. If the energy of the atoms or molecules in the pockets is less than that of the potential barrier at its maximum height, then the atoms are confined within the pockets of the optical lattice.

There are two important parameters associated with optical lattices. The first is the periodicity of the potential landscape. By changing the wavelength of the lasers, one can change the distance between neighboring atoms or molecules in the lattice. The second parameter of an optical lattice is its potential depth, which can be altered by adjusting the power of the laser beams. Both parameters give the experimentalist precise control over the atoms or molecules that are trapped in the pockets of the lattice. Optical lattices conveniently allow us to set up artificial barriers for which tunneling is favorable, by simply adjusting the parameters of the lattice, so that we may compare experimental results with quantum predictions.

The standing wave optical lattice is constructed using two counter-propagating laser beams of equal amplitude and wavelength. When the two beams meet, they interfere with one another. Figure 3.1 shows the standing wave potential of such a pair of interfering laser beams. By superimposing two or three orthogonal standing waves, we can obtain two- and three-dimensional periodic potentials. Each standing wave potential is given by

$$V(x) = V_0 \left(1 - \cos\left(\frac{\pi x}{D}\right)\right) \quad (3.1)$$

where D is the length period, which is half the wavelength of the laser light and V_0 is the potential depth of the lattice.

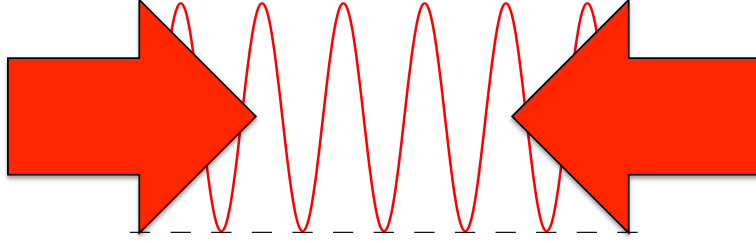


Figure 3.1: One-Dimensional Optical Lattice

3.2 The Lorentz Model

The Lorentz model provides a simple way to classically visualize the atom-field interaction. Imagine a neutral atom, whereby a tiny electron of mass m_e is attached to a heavy nucleus by an imaginary spring. The mass-spring system would then have a natural oscillation frequency ω_0 . Now, if that atom is placed in an external laser field, the oscillating electric field $\mathcal{E}(t)$ provides a driving force that displaces the negatively charged electron relative to the positively charged nucleus due to its interaction with the constituents of the neutral atom. Meanwhile, as this is happening, the imaginary spring exerts a restoring force, which is actually the attractive force between the nucleus and electron, on the electron mass. If it were not for this restoring force, the atom would break apart. From Newton's second law, the net force acting on the electron is the sum of the restoring force and the driving force

$$m_e \ddot{x}(t) = -m_e \omega_0^2 x(t) - e \mathcal{E}(t), \quad (3.2)$$

where e is the magnitude of the charge of the electron. If the electric field is a plane wave that oscillates with frequency ω_L , then the laser field can be written as $\mathcal{E}(t) = \mathcal{E}_0 \cos \omega_L t$. The solution to equation (3.2) is

$$x(t) = x_0 \cos \omega_L t,$$

where

$$x_0 = \frac{e \mathcal{E}_0}{m_e (\omega_L^2 - \omega_0^2)} \approx \frac{e}{2m_e \omega_0} \frac{\mathcal{E}_0}{\omega_L - \omega_0};$$

therefore, the net effect is that the electron will oscillate relative to the nucleus. The approximation used above assumes that the laser's frequency ω_L is close to the natural oscillating frequency ω_0 of the electron, and is given by

$$\omega_L^2 - \omega_0^2 = (\omega_L + \omega_0)(\omega_L - \omega_0) \approx 2\omega_0(\omega_L - \omega_0).$$

Since the external field \mathcal{E}_0 acts to stretch the atom, the separation of the electron from the nucleus causes the neutral atom to become polarized. The dipole moment is given by

$$P_0 = -\frac{e^2}{2m_e\omega_0} \frac{\mathcal{E}_0}{\omega_L - \omega_0} = \alpha\mathcal{E}_0, \quad (3.3)$$

which introduces a polarizability α . The energy of the dipole in the electric field is given by

$$\Delta E = -P_0\mathcal{E}_0/2 = -\frac{\alpha}{2}|\mathcal{E}_0|^2 = \frac{1}{2} \frac{(e^2/2m_e\omega_0)}{\omega_L - \omega_0} |\mathcal{E}_0|^2,$$

which is linear to the intensity $|\mathcal{E}_0|^2$ and inversely proportional to the detuning $(\omega_L - \omega_0)$.

If the intensity is a function of position, this shift gives rise to a position-dependent potential $U(\mathbf{r}) \sim |\mathcal{E}_0(\mathbf{r})|^2/(\omega_L - \omega_0)$.

3.3 Optical Lattices

Now considering the potential induced by the standing wave pattern of counter-propagating laser beams, the laser field is the superposition of the two waves, i.e.

$$\mathcal{E}_0(\mathbf{r}) = \frac{\mathcal{E}_0}{2} [e^{i\mathbf{k}_L \cdot \mathbf{r}} + e^{-i\mathbf{k}_L \cdot \mathbf{r}}] = \mathcal{E}_0 \cos(\mathbf{k}_L \cdot \mathbf{r}).$$

If the two laser beams are directed along the z -axis, the potential is given by

$$U(\mathbf{r}) \sim \frac{|\mathcal{E}_0(\mathbf{r})|^2}{(\omega_L - \omega_0)} = \frac{\mathcal{E}_0^2}{(\omega_L - \omega_0)} \cos^2(k_L z) = \frac{\mathcal{E}_0^2}{2(\omega_L - \omega_0)} [\cos(2k_L z) + 1].$$

Consider a laser beam of wavelength λ_L that is guided into a Gaussian beam. One important parameter regarding the beam is the waist size, which is the smallest radial distance that the beam intensity drops by some fractional amount of its maximum intensity. Using the $1/e$ convention (i.e., the radius at which the beam intensity drops by a factor of $1/e$ of its axial value) to describe the beam's waist σ_x and σ_y , diffraction theory predicts an intensity variation of the form

$$|\mathcal{E}(\mathbf{r})|^2 = |\mathcal{E}_0|^2 \exp\left[-2\left(\frac{x^2}{\sigma_x^2} + \frac{y^2}{\sigma_y^2}\right)\right] \left[1 + \left(\frac{z\lambda_L}{\pi\sigma_x^2}\right)^2\right]^{-1} \left[1 + \left(\frac{z\lambda_L}{\pi\sigma_y^2}\right)^2\right]^{-1}.$$

Assuming that the laser beam forming the optical lattice is focussed and tuned at a frequency for which the atoms are attracted to the high intensity (focal point) region (i.e., $\omega_L < \omega_0$), so that the beam can be used to trap the neutral atoms that placed in its path. If the beam is also assumed to have cylindrical symmetry, then $\sigma_x = \sigma_y$ and then the atoms experience a potential of the form

$$U(\mathbf{r}) = -\frac{U_0}{2} \frac{[\cos(2k_L z) + 1]}{\left[1 + \left(\frac{2z\lambda_L}{\pi\sigma^2}\right)^2\right]^2} e^{-\rho^2/\sigma^2},$$

where $\boldsymbol{\rho} = (x, y)$.

In a region outside the depth of focus, say near z_0 , the potential is

$$U(\mathbf{r}) = -\frac{\mathcal{U}_0}{2} [\cos(2k_L z) + 1] e^{-\rho^2/\sigma^2}, \quad (3.4)$$

where $z_0 \gg \pi\sigma^2/2\lambda_L$ and $\mathcal{U}_0 = U_0/(2z_0\lambda_L/\pi\sigma^2)^2$. It is apparent from (3.4) that the lattice potential has periodic minima occurring when $2kz \simeq \pi + 2\pi n$ is satisfied, and decays as the radial distance from the beam's axis of symmetry increases. Considering a local potential minima on the symmetry axis of the beam (i.e., $x = y = 0$), an atom placed in the pocket would experience a potential

$$U(z) \simeq -\frac{\mathcal{U}_0}{2} \frac{(2k_L z)^2}{2} = \mathcal{U}_0 k_L^2 z^2 = m\omega_{opt}^2 z^2, \quad (3.5)$$

where the Taylor expansion about $z = \pi$ has been used to approximate the cosine term in (3.4). As suggested by (3.5), the potential in the local minima acts like a harmonic oscillator with frequency

$$\omega_{opt} = \sqrt{2 \frac{\mathcal{U}_0}{\hbar} \frac{\hbar k_L^2}{2m}} = \sqrt{2b} \omega_r,$$

where $\omega_r = \hbar k_L^2 / 2m$ is the recoil frequency, and b represents the height of the potential barrier, $\mathcal{U}_0 = b\hbar\omega_r$.

3.4 Application

One application of an optical lattice is to form Feshbach molecules. Since we are able to trap unbound atoms within each pocket of the lattice, we can control the interaction between two atoms by tuning an external magnetic field, thus creating a single molecule at Feshbach resonance.

Chapter 4

FESHBACH MOLECULES

4.1 Scattering

A property of waves is that all points on a wavefront can be thought of as point sources for secondary wavelets. Let's consider a beam of incoming particles approaching a nucleus. When the beam enters a region where it interacts with the target nucleus, it experiences a short range potential $V(r)$ - for simplicity sake, consider the nucleus to have a spherically symmetric potential. Since we can represent the particle beam as a plane wave, then when the incoming plane wave scatters off of the localized scattering center, outgoing spherical waves are produced at the target site. Our problem now becomes a matter of finding the angular distribution of the scattered particles. Since the sensors used to detect the outgoing particles will be very far from the scattering center, as compared to the dimensions of the particles, we may take $r \rightarrow \infty$. At such distances, the scattered particles no longer feel the presence of the potential and our solution should be an incoming plane wave and an outgoing spherical wave of scattered particles of the form

$$\psi \sim e^{ikz} + f(\theta) \frac{e^{ikr}}{r}, \quad (4.1)$$

where the incident plane wave is traveling along the z-axis, and $f(\theta)$ is known as the scattering amplitude. As suggested by equation (4.1), the scattering amplitude has a dependence on the angle θ , which is formed by the asymptotic line to the path of the scattered particles and the incident particle beam.

4.1.1 Differential Cross Section

An incident beam of particles approaching a scattering center will be deflected due its interaction with the target. Let's consider for the moment a beam of particle approaching a scattering center. If we place an imaginary line that runs through the scattering center and is also parallel to the beam, then we can create a quantity called the impact parameter b , which is the perpendicular distance of the beam from that imaginary line. In general, the smaller the impact parameter, the more the beam is scattered from its incident path. If we

now call this imaginary line our z-axis and center an imaginary surface on and perpendicular to this axis, then our beam will penetrate a small patch of area $d\sigma$ a distance b from its center. This scattering angle θ is the angle between the asymptotic line that the scattered beam emerges from and our z-axis. If we place a unit sphere about the target, then the infinitesimal area that the scattered beam penetrates will be equivalent to the differential solid angle $d\Omega$. The differential cross section is defined as

$$\frac{d\sigma}{d\Omega} = \frac{dN/d\Omega}{n\Phi}, \quad (4.2)$$

where Φ is the incident flux (i.e., the number of particles per unit area, per unit time) entering into area $d\sigma$, dN is the number of particles detected in $d\Omega$, and n is the number of scattering centers in the target. The solid angle is defined as $d\Omega = \sin\theta d\theta d\phi$, but reduces to $d\Omega = 2\pi \sin\theta d\theta$ if the scattering potential has spherical symmetry.

The probability current,

$$\mathbf{j} = \frac{\hbar}{m} \text{Im}(\Psi^* \nabla \Psi), \quad (4.3)$$

will be now employed in the definition of a function that measures the angular distribution of the particles scattered by $V(r)$. For the incident plane wave the current is

$$j_i = \frac{\hbar}{m} \text{Im} \left(e^{-ikz} \frac{d}{dz} e^{ikz} \right) = \frac{\hbar k}{m} = v \quad (4.4)$$

and for the outgoing spherical wave

$$j_r \sim \frac{\hbar}{m} im \left\{ f^*(\theta) \frac{e^{-ikr}}{r} \frac{\partial}{\partial r} \left[f(\theta) \frac{e^{ikr}}{r} \right] \right\} = \frac{v}{r^2} |f(\theta)|^2. \quad (4.5)$$

$d\sigma/d\Omega$ has the dimension of area and its value is obtained from

$$\frac{d\sigma}{d\Omega} = \frac{j_r r^2}{j_i}, \quad (4.6)$$

by the fact that the number of particles that cross a given area per unit time is measured by the probability current flux through that area. Using (4.4) it is clear that

$$\frac{d\sigma}{d\Omega} = |f(\theta)|^2, \quad (4.7)$$

being thus the determination of the angular distribution reduced to the evaluation of the scattering amplitude $f(\theta)$.

The *total cross section* is obtained by integrating (4.7):

$$\sigma = \int \frac{d\sigma}{d\Omega} d\Omega = 2\pi \int_{-1}^{+1} |f(\theta)|^2 d(\cos \theta) \quad (4.8)$$

and its meaning is obvious: the total cross section measures the number of events per target nucleus per unit time divided by the incident flux defined above.

4.1.2 Partial waves

Since spherically symmetric potentials $V(r)$ are of interest to us, the solutions of the time-independent Schrödinger equation

$$-\frac{\hbar^2}{2m} \nabla^2 \psi + V\psi = E\psi \quad (4.9)$$

can be expressed as a linear combination of the product of the radial and angular parts

$$\psi(r, \theta, \phi) = \sum_{l,m} a_{lm} \frac{u_l(r)}{kr} Y_l^m(\theta, \phi), \quad (4.10)$$

where $k = \sqrt{2mE}/\hbar$, Y_l^m is a spherical harmonic, and $u_l(r) \equiv rR_l(r)$ is a solution of the radial equation

$$-\frac{\hbar^2}{2m} \frac{d^2 u_l}{dr^2} + \left[V(r) + \frac{\hbar^2}{2m} \frac{l(l+1)}{r^2} \right] u_l = E u_l. \quad (4.11)$$

A necessary condition that we must place on u , so that it doesn't explode at the origin, is that $u_l(0) = 0$.

Since our problem has rotational symmetry, we can further simplify our problem by setting $m = 0$ and eliminating any dependence on ϕ ; therefore, reducing equation (4.10) to

$$\psi(r, \theta) = \sum_l a_l \frac{u_l(r)}{kr} P_l(\cos \theta). \quad (4.12)$$

The terms of (4.12) can be understood as *partial waves*, from which the general solution Ψ can be constructed. It is also useful to present the plane wave by an expansion in Legendre polynomials

$$e^{ikz} = e^{ikr \cos \theta} = \sum_{l=0}^{\infty} (2l+1) i^l j_l(kr) P_l(\cos \theta), \quad (4.13)$$

where $j_l(x)$ are spherical Bessel functions and $P_l(\cos \theta)$ the Legendre polynomials.

At large distances from the origin the spherical Bessel functions reduce to the simple expression

$$j_l(kr) \sim \frac{\sin(kr - \frac{l\pi}{2})}{kr} = \frac{e^{i(kr - \frac{l\pi}{2})} - e^{-i(kr - \frac{l\pi}{2})}}{2ikr}. \quad (4.14)$$

Using (4.14) in (4.13) results in

$$e^{ikr \cos \theta} \sim \frac{1}{2i} \sum_{l=0}^{\infty} (2l+1) i^l P_l(\cos \theta) \left[\frac{e^{i(kr - \frac{l\pi}{2})} - e^{-i(kr - \frac{l\pi}{2})}}{kr} \right], \quad (4.15)$$

that represents the asymptotic form of a plane wave.

In (4.15) the first term inside brackets corresponds to an outgoing spherical wave and the second to an ingoing spherical wave. Thus, each partial wave in (4.15) is, at large distances from the origin, a superposition of two spherical waves, an ingoing and an outgoing. The total radial flux for the wavefunction $\Psi_i = e^{ikr \cos \theta}$ vanishes, since the number of free particles that enters into a region is the same that exits. This can be easily shown using (4.15) in (4.3).

Let us now understand Ψ in (4.12) as a solution of a scattering problem, the scattering being caused by a potential $V(r)$. The asymptotic form of Ψ can be obtained if we observe that the presence of the potential has the effect to cause a perturbation in the outgoing part

of the plane wave, and such perturbation can be represented by a unitary module function, $S_l(k)$.

From (4.15), this leads to

$$\Psi \sim \frac{1}{2i} \sum_{l=0}^{\infty} (2l+1) i^l P_l(\cos \theta) \frac{S_l(k) e^{i(kr - \frac{l\pi}{2})} - e^{-i(kr - \frac{l\pi}{2})}}{kr}, \quad (4.16)$$

where the function $S_l(k)$ can be represented by

$$S_l(k) = e^{2i\delta_l}. \quad (4.17)$$

From a comparison of (4.16) and (4.12) we can obtain the expressions for a_l and for the asymptotic form of $u_l(r)$:

$$a_l = i^l (2l+1) e^{i\delta_l} \quad (4.18)$$

and

$$u_l(r) \sim \sin \left(kr - \frac{l\pi}{2} + \delta_l \right). \quad (4.19)$$

$u_l(r)$ differs from the asymptotic form of the radial function of a free particle by the presence of the *phase shifts* δ_l ; the presence of the scattering potential creates in each partial wave a phase shift δ_l and the scattering problem would be solved with the determination of these phase shifts for a given potential $V(r)$. In fact, the use of (4.16) and (4.15) results in

$$f(\theta) = \frac{1}{k} \sum_{l=0}^{\infty} (2l+1) e^{i\delta_l} \sin \delta_l P_l(\cos \theta) \quad (4.20)$$

and the differential cross section (4.7) is obtained from the knowledge of the phase shifts δ_l . The phase shifts are evaluated by solving equation (4.11) for each l and comparing the phase of $u_l(r)$, for some large r , with the phase of $j_l(kr)$ for the same value of r .

The total cross section has the expression

$$\sigma = \frac{4\pi}{k^2} \sum_l (2l+1) \sin^2 \delta_l, \quad (4.21)$$

obtained by the integration (4.8).

The partial wave expansion is useful only at low energies since in this case the number of terms of (4.20) that we have to deal is small. If the energy is low enough, the sum (4.20) reduces to the term with $l = 0$. We have, in this case,

$$f(\theta) = \frac{1}{k} e^{i\delta_0} \sin \delta_0 \quad (4.22)$$

and

$$\sigma = \frac{4\pi}{k^2} \sin^2 \delta_0. \quad (4.23)$$

The differential cross section that results from (4.22) is independent of θ : the scattering is isotropic. This is easily understandable since at low energies the incident particle wavelength is much greater than the dimension of the target nucleus; during its passage all points in the nucleus are with the same phase at each time and it is impossible to identify the direction of incidence.

In the extreme case $E \rightarrow 0$ the scattering amplitude (4.22) remains finite only if $\delta_0 \rightarrow 0$ together with the energy. In this case the phase difference is no more the main scattering parameter. A better parameter is the *scattering length* a , defined as the limit

$$\lim_{E \rightarrow 0} f(\theta) = \lim_{k \rightarrow 0} \frac{\delta_0}{k} = -a, \quad (4.24)$$

yielding the equation

$$\sigma = 4\pi a^2 \quad (4.25)$$

as the expression for the total cross section at the zero energy limit. A negative (positive) scattering length results in an overall attractive (repulsive) interaction. The magnitude and sign of the scattering length for a single potential are mainly determined by the highest bound state. If it is just below the continuum the scattering length is large and positive. The effective range of interactions is typically on the order of the spatial range of the interatomic potential.

The validity of the result above is justified in the weakly interacting limit ($ka \ll 1$), whereas in the strongly interacting limit (strong resonances), $\delta_0 = \pi/2$, $\sin \delta_0 = 1$, the scattering cross section $\sigma(k) = 4\pi/k^2$ becomes independent of the scattering length. For a gas of interacting particles, it is proportional to the spread of the wave packet of the atom represented by the square of the de Broglie wave length

$$\lambda_{dB} = \sqrt{\frac{2\pi\hbar^2}{mk_B T}} \quad (4.26)$$

where k_B is the Boltzmann constant, T is the temperature of the gas and m the mass of the particles.

4.2 Feshbach Molecules

To understand the underlying principle of Feshbach resonances, consider two interatomic potentials for atoms in different spin states, as shown in figure 4.1). Each potential is referred to as a scattering channel. The incoming atoms scatter in the lower potential also named an *open channel*. The incoming atoms have very low kinetic energy and we assume that they enter in the open channel close to the molecular dissociation threshold. The upper potential is typically referred to as the closed channel because it is energetically not accessible at large distances between the atoms. The highest levels of the closed channel can lie above the continuum of the open channel. The scattering properties are altered by the coupling of both channels. If the closed channel supports a bound state with an energy that is close to the energy of the incoming atoms, this bound state can temporarily be populated during the scattering process provided that the Hamiltonian can flip the atomic spins. In other words, a bound state of the closed channel just below the continuum of the open channel gives rise to a large positive scattering length. Similarly, a virtual bound state just above the continuum yields a large and negative scattering length. The energy difference between the bound state and the open-channel dissociation threshold is denoted by ΔE . If $\Delta E \rightarrow 0$, the population of the bound state is resonantly enhanced (for a discussion on resonant tunneling, see chapter 1) and a Feshbach resonance occurs. Here, a resonance state means a short-lived bound state, existing long enough for participating in other scattering processes.

The key idea to construct Feshbach molecules is that, the scattering channels have different spins and, therefore, they also have different magnetic moments. This can be used to tune ΔE by applying a magnetic field. If the molecular resonant state has a different magnetic moment to that of the free atoms, an external magnetic field shifts the potentials with respect to each other. Hence, by applying a magnetic field it may be possible to bring a bound state of the closed channel into degeneracy with the continuum giving rise to a Feshbach resonance. At the position of the Feshbach resonance the scattering length diverges. The scattering channels typically have different spins and, therefore, they also have different magnetic moments. Thus, the magnetic field can be used to tune ΔE . Close to $\Delta E = 0$ a linear approximation holds

$$\Delta E = \Delta\mu(B - B_0), \quad (4.27)$$

where, $\Delta\mu = \mu_b - 2\mu_a$ denotes the difference in magnetic moment between the bound state μ_b and two atoms $2\mu_a$ and B_0 is the magnetic field value where $\Delta E = 0$.

In the case of *s*-wave scattering, and close to resonance, the coupling of the free atom-pair state to the bound state strongly modifies the scattering properties of the free atoms and the magnetic field dependence of the scattering length is

$$a(B) = a_f \left(1 - \frac{\Delta}{B - B_0 + i\hbar\Gamma/2\Delta\mu} \right). \quad (4.28)$$

This means that, far away from the resonance ($B \gg B_0$), the scattering length approaches its free value a_f . The magnetic field width of the resonance is denoted by Δ . The total decay rate of the population in the bound state into all open channels is Γ , with a lifetime equal to $\tau = \hbar/\Gamma$.

It is usual to distinguish between broad and narrow Feshbach resonances. Broad Feshbach resonances are characterized by $k_F r_0 \ll 1$, where $k_F = \sqrt{2mE_F/\hbar^2}$ is the Fermi momentum (E_F is the Fermi energy), which depends on the density of the atomic gas, and r_0 is the approximate range of the inter-atomic potential.

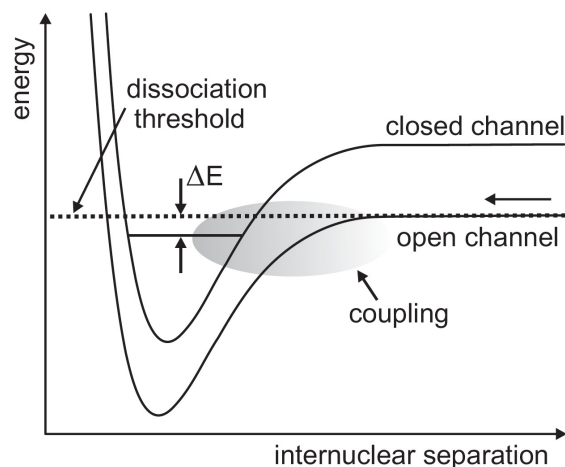


Figure 4.1: Due to the different magnetic moments the closed channel can be shifted relative to the open channel by applying a magnetic field. Tuning a bound state of the closed channel to degeneracy with the continuum of the open channel leads to a Feshbach resonance.

The main idea is shown to create a Feshbach molecule is shown in figure 4.2. The dependence of energy on the magnetic field is depicted for the free atoms in the open channel and the bound state in the closed channel. Due to an avoided crossing (avoided crossings are explained in Chapter 1) the molecular state below the resonance is connected to the free atom state above the resonance. The Feshbach molecule above the resonance is unstable and is hence referred to as a virtual bound state. To associate molecules, two atoms are first prepared at a magnetic field above the Feshbach resonance in the lowest state. A subsequent modification of the magnetic field across the Feshbach resonance transfers population into the bound state by adiabatically following the lower branch of the avoided crossing as indicated by the arrow in figure 4.2. The magnetic field value at the end of the process determines the binding energy. For slow variations of the magnetic field, the molecule formation (also called *association* process) efficiency approaches 100%. It is characteristic that these Feshbach molecules in the s-wave channel are only very weakly bound. The binding energy E_B of these molecules represents the energy difference between the lowest molecular and atomic states.

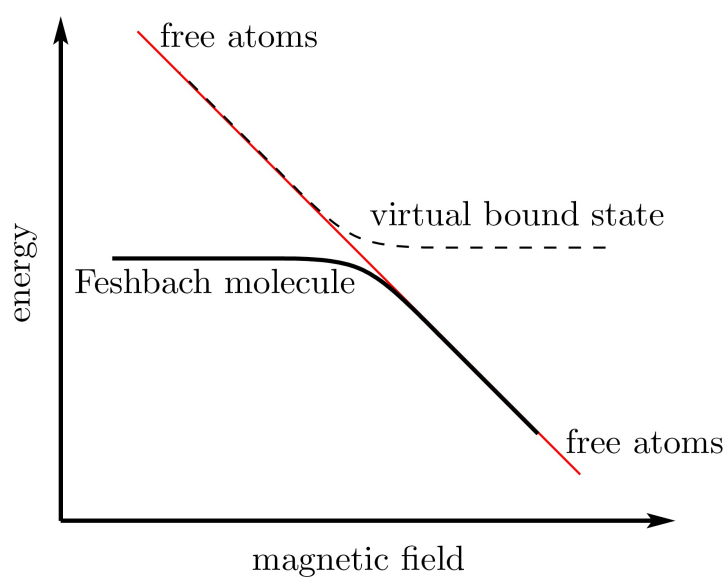


Figure 4.2: Due to the different magnetic moments the closed channel can be shifted relative to the open channel by applying a magnetic field. Tuning a bound state of the closed channel to degeneracy with the continuum of the open channel leads to a Feshbach resonance.

Chapter 5

TUNNELING, DIFFUSION AND DISSOCIATION OF FESHBACH MOLECULES IN OPTICAL LATTICES

The quantum dynamics of an ultra-cold diatomic molecule, tunneling and diffusing in a one-dimensional optical lattice exhibits unusual features. While it is known that the process of quantum tunneling through potential barriers can break up a bound state molecule into a pair of dissociated atoms, interference and re-association produce intricate patterns in the time evolving site-dependent probability distribution for finding atoms and bound-state molecules. We find that the bound-state molecule is unusually resilient against break up at ultra-low binding energy E_b (E_b much smaller than the barrier height of the lattice potential). After an initial transient, the bound state molecule spreads with a width that grows as the square root of time. Surprisingly, the width of the probability of finding dissociated atoms does not increase with time as a power law.

5.1 Introduction

Ultracold atoms in optical lattices provide a versatile tool for the experimental study of many-body quantum dynamics, with an unprecedented degree of accessibility Lewenstein & Liu (2011). Quantum many-body properties of cold atom gases such as Bose-Einstein condensates and ultracold fermions Bloch & Zwerger (2008) are now studied in confining traps. Using the standing wave patterns of reflected laser beams, the ultra-cold atoms can experience a lattice potential of variable potential height Greiner & Fölling (2008), providing a laboratory for realizing the effective hamiltonians of strongly coupled electron physics Sachdev (2008) and for studying tunneling physics Arimondo & Wimberger (2011). Recent experiments have demonstrated that cold atom experimentalists can now observe individual atoms in an optical lattice with single site resolution Greiner & Fölling (2008). The traps can realize systems of reduced dimensionality Görlitz et al. (2001). These developments allow for unparalleled tests of fundamental quantum dynamics such as quantum diffusion, interference and localization in lattice potentials. In view of the condensed matter backdrop, the literature is rich on transport phenomena of particles in periodic lattices found in crystals, quasi-crystals and metals. Examples are Bloch oscillations of atoms due to the repeated

Bragg scattering in tilted periodic potentials as reported in Ref. Ben Dahan et al. (1996), and the shape of the quantum diffusion front in one-dimensional quasi-periodic systems studied in Ref. Zhong et al. (2001).

Combining the technique of Feshbach resonant Feshbach (1958) manipulation by tuning the strength of an external magnetic field Chin et al. (2010), Grimm’s group succeeded in associating pairs of optical lattice atoms trapped at the same site into bound state diatomic molecules of ultra-low and tunable binding energy Thalhammer et al. (2006). In this paper, we investigate the dynamics of tunneling, diffusion and tunneling-induced dissociation of ultracold diatomic molecules with a binding energy comparable to or smaller than the barrier height of the lattice potential. For quantum tunneling through a single barrier, composite particles are predicted to exhibit deviations from the exponential decay law. This quantum dynamics depends strongly on the intrinsic (composite particle) structure as the binding energy decreases Bertulani et al. (2007). We study the diffusion of a Rydberg like (with ultra-low binding energy) molecule with fine-tuned binding energy in a one-dimensional periodic lattice. In the process of quantum tunneling through a barrier, the molecule can dissociate into a pair of atoms that experience the same lattice potential.

The tunneling, diffusion, and dissociation properties of composite particles in periodic lattices is a subject of increasing interest Orso et al. (2005); Wouters & Orso (2006); Tsuchiya & Ohashi (2008). The combined quantum tunneling, interference and dissociation can be used as a tool to prepare and exploit the properties of the intrinsic molecular structure and the population of bound and continuum states through the controlled diffusion of molecules in periodic potentials. The calculations reported in this article predict a universal behavior for the long time evolution of the spreading width of molecular and atomic wavepackets as they are affected by the reflection, tunneling and diffusion process. Optical lattices are unique systems in this aspect, as they provide periodic barriers to study relevant quantum problems that no other known experimental setup can provide.

In references Orso et al. (2005); Wouters & Orso (2006); Tsuchiya & Ohashi (2008), a treatment of molecular diffusion in one-dimensional optical lattices has been carried out. Instead of a “prepared” initial state, an exact bound state solution is obtained for the same

Hamiltonian used in our work. This approach contrasts with ours, where we use a molecular wave function in a uniform gas as the initial state. In principle, our results should agree in the limit of tightly bound molecule, but it should be considered as an approximation for a weakly bound molecule. It is well-known that when the initial bound state is not an exact eigenstate, the time evolution is affected. Thus, the conclusions drawn from our work are limited to the extent that only a prepared, localized, initial state is considered. A localized state has high energy components, which tend to facilitate tunneling and diffusion. We thus expect that our obtained tunneling and diffusion times are essentially larger than those obtained for an exact solution of the initial state for an optical lattice.

Our study is simplified on purpose, as we want to learn about the fundamental aspects of diffusion of composite objects, subject to transforming transitions from bound to continuum states. The optical lattice potential has the form of a sine function with a periodicity that is the lattice constant D , equal to half the wavelength of the interfering laser, giving $D = 0.2 - 5 \mu m$ (the longer wavelengths are accessible with a Carbon dioxide lasers, for instance). Experimentally, the binding energy of a Feshbach molecule is tuned up by a magnetic field \mathbf{B} that controls the scattering length a . According to equation (4.28), this length varies with the magnetic field strength B as (for simplicity we use $\Gamma = 0$, assuming very narrow resonances)

$$a = a_{bg} \left[1 - \frac{\Delta}{(B - B_0)} \right], \quad (5.1)$$

where a_{bg} denotes the background scattering length, i.e. the value of the scattering length far from resonance. B_0 represents the on-resonance magnetic field, and Δ is the resonance width. For most known resonances, Δ takes on a value between 1 mGauss - 10 Gauss. The scattering length a can be varied from $a_{bg} \sim \text{nm}$ to several microns Donley et al. (2001). Near the resonance, the binding energy of the binary system of reduced mass μ and scattering length a are related by $E_b = \hbar^2/\mu a^2$, so that

$$\nu_b = \frac{E_b}{h} = \frac{h}{4\pi^2\mu a^2}. \quad (5.2)$$

For diatomic Rubidium-87 molecules, $\mu = Am_N/2$, where m_N is the nucleon mass and the atomic number $A = 87$. The numerical value of the constant of circulation h/m is equal to $h/m = 8.0/(A/100)\mu m^2/ms$, and the binding frequency is

$$\nu_b = \frac{1}{(\pi^2 A/100)} \frac{\text{kHz}}{(a/\mu\text{m})^2}. \quad (5.3)$$

Thus, for $a \sim 10$ nm and larger, typical binding energies are of the order of MHz, although very close to the resonance a binding energy of a few Hz can be achieved Krems et al. (2009). We will use binding energies in the range of kHz to study the dissociation and diffusion dependence on the molecule binding.

We now describe a method developed by Bailey et al. (2010). We consider a molecule consisting of two identical Rubidium-87 atoms. The Hamiltonian for the system interacting with the optical lattice, is given by $H = T_1 + T_2 + V_1 + V_2 + v$ where T_i is the kinetic energy of atom i , V_i is the periodic potential of the lattice, given by

$$V_i = V_0 \left[1 - \cos\left(\frac{\pi x_i}{D}\right) \right], \quad (5.4)$$

and v is the interaction potential between the atoms. The position of each atom within the lattice is given by x_i and $\mu = m_{Rb}/2$ is the reduced mass of the diatomic system. The inter-atom potential is assumed to be governed by the magnetic field near a Feshbach resonance, which is directly related to a positive scattering length a . As we only consider a single bound state regulated by the scattering length, we assume a Dirac-delta potential of the form $v(x_{12}) = -(2\pi\hbar^2/\mu a)\delta(x_{12})$, where $x_{12} = x_1 - x_2$. This potential holds a bound state at energy $E_b = -\hbar^2/2\mu a^2$ with wavefunction

$$\psi(x_{12}) = \sqrt{k} \exp(-k|x_{12}|), \quad \text{with } k = \sqrt{-2\mu E_b/\hbar^2}. \quad (5.5)$$

After preparing the initial state with a bound state molecule localized within one of the lattice sites, we calculate the tunneling, diffusion, and dissociation properties of the Feshbach molecule. Taking the center of the initially occupied lattice site as the origin, the

initial wavefunction is written as $\Psi_0(x, y) = \psi(x_{12})\Phi(x_s)$, where $x_s = (x_1 + x_2)/2$ is the center of mass of the molecule, and

$$\Phi(x_s) = \frac{1}{(2\pi\sigma_0^2)^{1/4}} \exp\left[-\frac{x_s^2}{4\sigma_0^2}\right], \quad (5.6)$$

is a normalized Gaussian wavepacket centered on the origin and localized with initial width σ_0 .

We calculate the wavefunction of the two atoms in a spatial grid for the x_1 and x_2 coordinates, so that $x_i^{(j)} = j\Delta x$, with $j = 1, 2, \dots, N$. The wavefunction $\Psi(x_1, x_2, t)$ is represented by the finite set of time-dependent functions $\Psi(x_1^{(i)}, x_2^{(j)}, t) = \Psi_{jk}(t)$ at the points $(x_1^{(1)}, x_2^{(2)})$ of the spatial grid. The derivations in the kinetic operators of Hamiltonian are approximated by three-point formulae. For the boundary conditions on the far left or far right of the grid we set $\Psi_{j0} = \Psi_{jN} = \Psi_{0k} = \Psi_{Nk} = 0$.

The time-evolution of the molecule wavefunction $\Psi(x_1, x_2, t)$ is obtained by solving the Schrödinger equation by a finite difference method. The wave function $\Psi(t + \Delta t)$ at time $t + \Delta t$ can be calculated from the wave function at time t , $\Psi(t)$, by applying the unitary time evolution operator, \mathbf{U} . In matrix notation for coordinates (x, y) ,

$$\Psi(t + \Delta t) = \mathbf{U}(t + \Delta t, t)\Psi(t). \quad (5.7)$$

For a small time step Δt between iterations, the time evolution operator can be approximated as

$$\mathbf{U}(t + \Delta t, t) \simeq \frac{1 + (\Delta t/2i\hbar) H(t)}{1 - (\Delta t/2i\hbar) H(t)}. \quad (5.8)$$

This is an implicit equation for the time evolution and is correct up to and including terms of the order $(\Delta t)^2$. It requires carrying out matrix multiplications and inversions at each iteration. The inversion is performed by an extension of the Peaceman-Rachford method and is well documented in the literature Varga (1962); Press et al. (2007). Appendix B shows how this procedure is implemented in practice.

To analyze the time evolving two-particle wavefunction Ψ , it is useful to distinguish the bound state molecule amplitude from that of dissociated atoms. The bound state molecule is associated with the projection of the two-particle wavefunction on the bound state wavefunction ψ of Eq. (5.5). The probability of finding a bound state molecule in the interval $(x_s - dx_s/2, x_s + dx_s/2)$ at time t is $P_M(x_s, t)dx_s$ where

$$P_M(x_s, t) = \left| \int dx_{12} \Psi(x_s - x_{12}/2, x_s + x_{12}/2, t) \psi^*(x_{12}) \right|^2. \quad (5.9)$$

The probability of finding a dissociated atom is the difference of two probabilities: the probability of finding an atom and the probability that this atom is part of a bound state molecule. We refer to the probability of finding a dissociated atom within an interval $(x - dx/2, x + dx/2)$ at time t as $P_A(x, t)dx$. As this atoms can be either atom 1 or atom 2, and as we have to subtract out the bound molecule probability, we obtain

$$\begin{aligned} P_A(x, t) = & \int dx_2 |\Psi(x, x_2, t)|^2 - \left| \int dx_2 \Psi(x, x_2, t) \psi^*(x - x_2) \right|^2 \\ & + \int dx_1 |\Psi(x_1, x, t)|^2 - \left| \int dx_1 \Psi(x_1, x, t) \psi^*(x_1 - x) \right|^2. \end{aligned} \quad (5.10)$$

In accordance with intuition - the dissociation of each molecule (in a statistical ensemble) produces two atoms - Eqs. (5.9) and (5.10) ensure that

$$\int dx \left[P_M(x, t) + \frac{P_A(x, t)}{2} \right] = \int dx_1 \int dx_2 |\Psi(x_1, x_2, t)|^2 = 1 \quad (5.11)$$

corresponding to a normalization condition satisfied by the atom/molecule probabilities.

We first consider the case of a tightly bound molecule for which little dissociation occurs. There is no coupling to the continuum, $P_A = 0$, and the P_M probability of a bound state molecule diffuses as a single particle in a quantum tunneling and diffusion process in the periodic potential. An illustrative example of $P_M(x, t)$ is shown in figure 5.1. The lattice constant D of the potential is equal to $D = 2 \mu\text{m}$ and the binding energy E_b of the bound

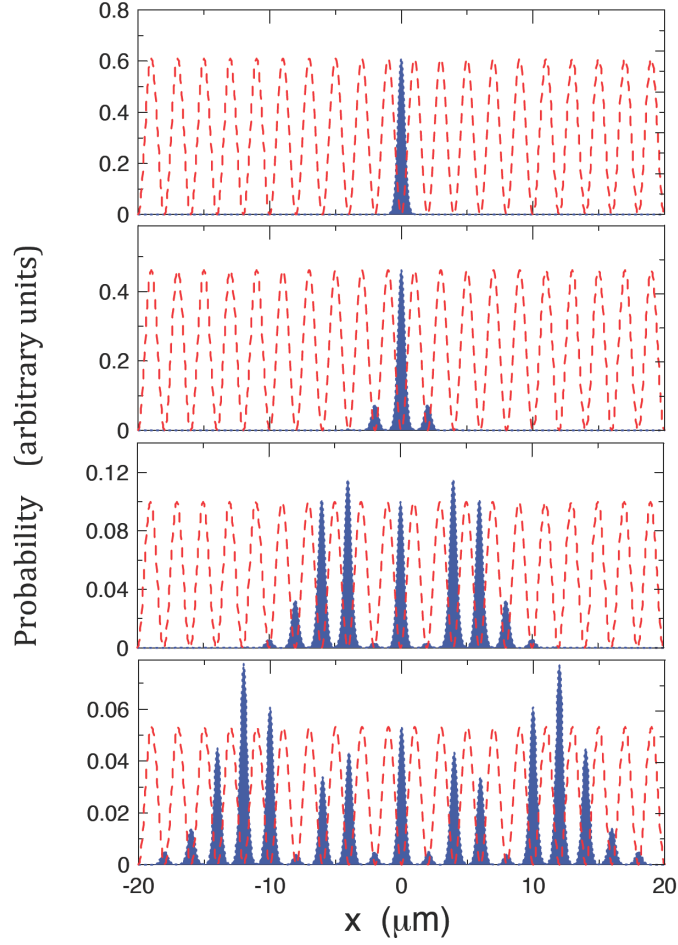


Figure 5.1: Time evolution of the probability distribution of strongly bound ($E_b = 10$ kHz) Rubidium molecules in an optical lattice with size $D = 2 \mu\text{m}$. From top to bottom the time is $t = 0$, $t = 10$ ms, $t = 25$ ms and $t = 100$ ms, respectively.

state molecule is given by $E_b = 10$ kHz. The potential barrier height V_0 and the width are chosen so that the molecule can easily tunnel through the barriers, $V_0 = 200$ Hz. The graphs show the probability of finding a molecule at position x after a time $t = 0$, $t = 10$ ms, $t = 25$ ms and $t = 100$ ms. For better visualization the barrier height is rescaled by a factor so that the height of the particle probability at the central position matches with the top of barrier. As expected, due to the exponential decay of the wavefunction within the barriers, the probability distribution peaks in the middle of the lattice sites. The initial wave packet, localized at the origin, leaks successively through each barrier. The interference of scattered and transmitted waves induces an increasing number of wave fronts to appear in the probability distribution as time evolves. The width of the probability distribution for

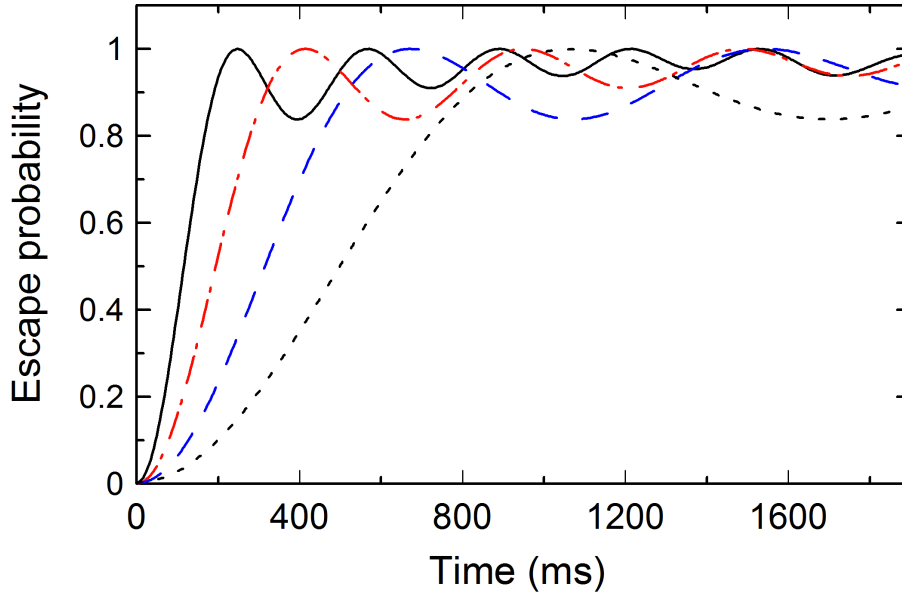


Figure 5.2: Time dependence of the escape probability of strongly bound Rubidium molecules from an optical lattice with size $D = 2 \mu\text{m}$, as a function of increasing potential barrier heights. The barrier height increases each time by a factor of 1.5 in going from the solid to dashed-dotted, from dashed-dotted to long-dashed, and from long-dashed to dotted curve.

finding a bound state molecule grows with increasing time. As a consequence of the mirror symmetry of the initial state and the Hamiltonian, the distribution function maintains mirror symmetry.

In figure 5.2 we show the time dependence of the escape probability - the probability that the molecule is not found in the initial lattice site - of the strongly bound Rubidium molecules of the previous calculation. The time dependence is plotted as a function of increasing potential barrier heights. The barrier height increases each time by a factor of 1.5 in going from the solid ($V_0 = 200 \text{ Hz}$) to dashed-dotted, from dashed-dotted to long-dashed, and from long-dashed to dotted curve. As expected, the escape probability increases at a slower pace if the barrier height is larger. After reaching a maximum value the escape probability oscillates due to reflections that feed back amplitude to the initial position.

We now consider the quantum diffusion of Rydberg molecules with low binding energy E_b , where $E_b < V_0$. In this regime, a molecule does not only diffuse by quantum tunneling through the barriers of the lattice, but can also dissociate into a pair of atoms in the process of tunneling and $P_A \neq 0$. Many notable examples of this physics with a single potential bar-

rier occur in nuclear fusion reactions (see e.g Refs. Bertulani et al. (2007); Bertulani (2011)). The probability that the atoms remain bound in the initial molecule state, $\int dx P_M(x, t)$, is called the “integrity”. In Fig. 5.3 we plot the time dependence of the integrity probability of Rubidium molecules as they tunnel and diffuse through an optical lattice with size $D = 2 \mu\text{m}$, and a fixed potential barrier height $V_0 = 5 \text{ kHz}$. The binding energies were parametrized in terms of the barrier height, with $E_4 = V_0/20$, $E_3 = V_0/5$, $E_2 = V_0/2$, and $E_1 = V_0/1.2$. While the center of mass of the two atoms is initially localized within a few μm , the atom/molecule probabilities spread over time. It is necessary to have a sufficiently large lattice to accommodate the P_A and P_M -probabilities. This is relatively easily achieved in one-dimensional calculations, but represents a computational challenge for calculations in higher dimensions. In some cases we work with a spatial mesh encompassing a few hundred of lattice sites to allow for convergence of the loosely-bound molecule amplitude.

As the binding energy of the molecules decreases from V_0 , the integrity probability initially reduces. In this regime, the tunneling rate increases with lower binding energy and tunneling favors dissociation, in line with previous studies in fusion reactions Bertulani et al. (2007); Bertulani (2011). The natural interpretation is that increased tunneling also increases the interactions of the individual atoms with a larger number of barriers, thus increasing the dissociation probability.

Despite the apparently obvious interpretation given above, the molecule is also resilient to breakup: even at the smallest binding value, the breakup probability is not that big. This interpretation loses meaning at very low binding energies, as seen by the case of $E_4 = V_0/20$, in which case the integrity increases relative to that cases 2 and 3 of higher binding energy. At that binding energy, the trend is reversed and the molecule tends to remain intact. This result is not unusual, as other tunneling systems exhibit similar behavior. Perhaps the most familiar example is the tunneling of a Cooper pair Brink et al. (1991). The pair does not usually dissociate as it tunnels through a barrier. However composite particles may dissociate as the particles tunnel through multiple barriers, as in the case of a lattice potential. Moreover, the binding mechanism of a Cooper pair is rather different from the inter-particle potential binding considered here.

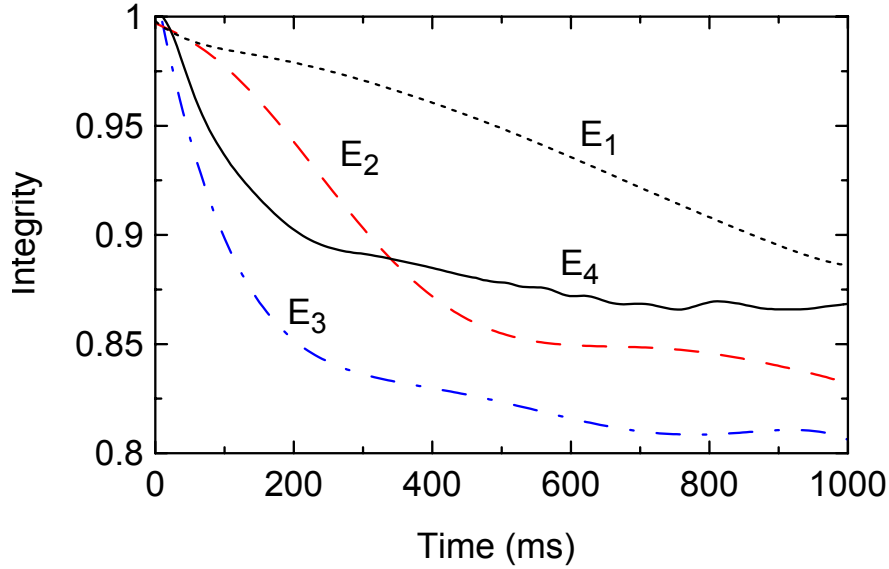


Figure 5.3: Time dependence of the “integrity” probability of loosely bound Rubidium molecules by tunneling and diffusion through an optical lattice with lattice constant $D = 2 \mu\text{m}$, and potential barrier height $V_0 = 5 \text{ kHz}$. The integrity is the probability that the molecule remains in its bound state. The binding energies were parametrized in terms of the barrier height, with $E_4 = V_0/20$, $E_3 = V_0/5$, $E_2 = V_0/2$, and $E_1 = V_0/1.2$.

In figure 5.4 we show the probability of finding the bound state molecule (hatched histograms) or of finding a dissociated atom (full histograms) in the different lattice sites for the case $E_b = 250 \text{ kHz}$ and $V_0 = 5 \text{ kHz}$ at two different times, $t_1 = 200 \text{ ms}$ and $t_2 = 400 \text{ ms}$. The time progression gives a sense of the quantum dynamics. The height of the hatched (bound molecule) histogram for site i , $P_{M,i}$, is equal to $P_{M,i} = \int_{[i-1/2]D}^{[i+1/2]D} dx P_M(x)$ whereas the height of the full (dissociated atom) histogram, $P_{A,i}$, gives the value of $P_{A,i} = \int_{[i-1/2]D}^{[i+1/2]D} dx P_A(x)$. Note that the diffusion front of the bound state molecule spreads with a larger speed than that of the dissociated atoms. Because it takes additional time for the molecules to dissociate, the atoms diffuse slower than the bound state molecules within the lattice. It takes time for the molecules to dissociate, and additional time for the atoms to diffuse after the dissociation. We thus predict that the molecules, initially confined within a lattice site, will tunnel and diffuse away from the initial position at a higher speed than the atoms that are created in the dissociation of the molecules.

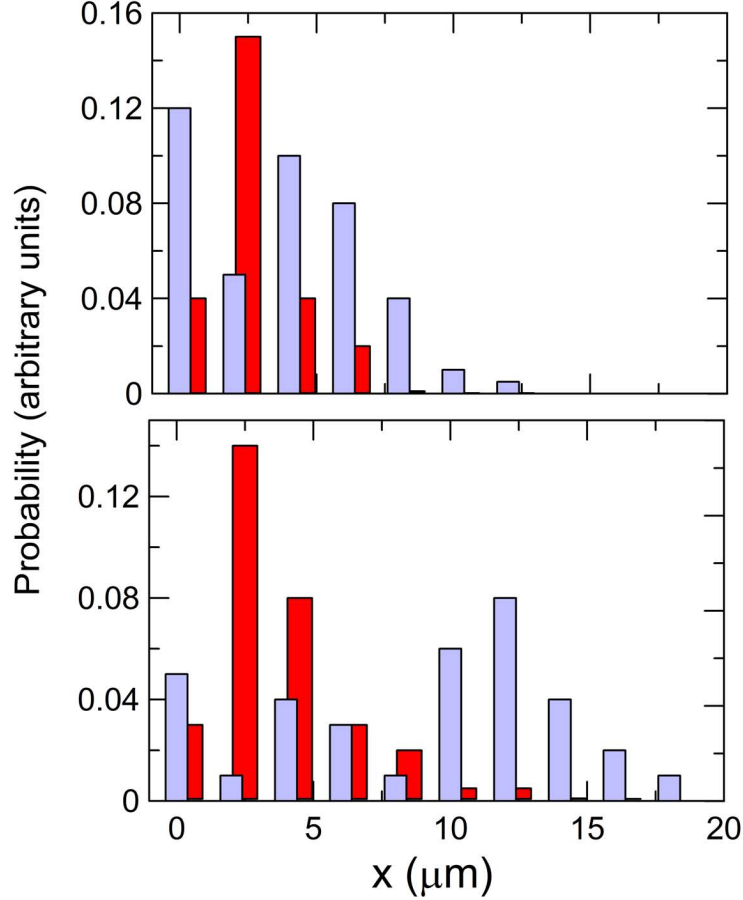


Figure 5.4: Lattice diffusion of molecules. The hatched histograms are the relative probability of finding a molecule in its ground state at a given position along the lattice. The solid histograms give the relative probability of finding individual atoms after the dissociation. This figure was generated for the highest dissociation probability (20%) described in figure 5.3.

We can characterize the speed of the wave front progression for bound state molecule diffusion in the lattice by calculating the width $\sigma(t) \equiv \sqrt{\langle r^2(t) \rangle}$, where the average is taken with respect to the bound state molecule distribution, when characterizing the bound state molecule diffusion,

$$\sigma_M(t) \equiv \sqrt{\int dx x^2 P_M(x, t) / \int dx P_M(x)}$$

and with respect to the dissociated atom distribution when characterizing the dissociated atom spreading,

$$\sigma_A(t) \equiv \sqrt{\int dx x^2 P_A(x, t) / \int dx P_A(x)}.$$

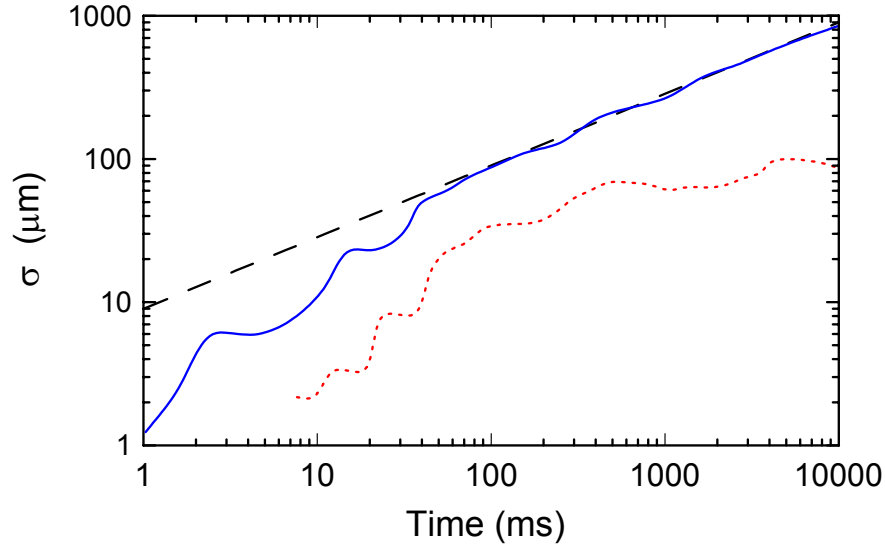


Figure 5.5: Time dependence of the spreading width of bound molecules, $\sigma_M(t)$, shown in solid line and of dissociated atoms, $\sigma_A(t)$, shown in dotted line, defined in the text. The dashed curve is a fit of the asymptotic time-dependence with the analytical formula, Eq. (5.15).

In the long-time regime, the molecule and atom distributions do not spread as fast as the probability of a single free particle quantum wavefunction does, $\sigma_{free} \sim \hbar t / (2M\sigma_0)$, where M is the mass of the particle and σ_0 is the initial width of the wave packet. In contrast, the distribution of the bound state molecule with low binding energy spreads as $\sigma_M(t) \sim t^{1/2}$ at long times, as shown in Fig. 5.5). The dissociated atoms spread more slowly still, although their width, shown in the dotted line, does not attain the form of a power law in time. Instead, the width appears to grow in steps becoming orders of magnitude smaller than the molecule width at long times. We also find a non-trivial correlation between $\sigma_A(t)$ and the molecule binding energy. Generally, molecules of lower binding energy exhibit a more complex time dependence of σ_A upon t .

The long-time power scaling $\sigma_M \sim t^{1/2}$ contrasts with the linear scaling of a free particle wave packet and of a Gaussian wave packet propagating in a tight-binding model Hamiltonian Korsch & Mossmann (2003), Klumpp et al. (2007) (if the lattice potential is not tilted). How can we understand the scaling of σ_M ? We can try to understand the long time particle diffusion through the lattice by using semiclassical arguments. Starting from a

time-dependent Schrödinger equation

$$i\hbar\partial_t\phi = -\hbar^2\partial_x^2\psi/2m + V\psi,$$

where V is the lattice potential, and writing the wavefunction as

$$\psi = \sqrt{\rho}\exp(iS/\hbar),$$

we get the semiclassical equation

$$m\frac{\partial v}{\partial t} + mv\frac{\partial v}{\partial x} = -\frac{\partial(V+U)}{\partial x} \quad (5.12)$$

where $v = \partial_x S/m$ is the measure of the particle velocity, and

$$U = -\hbar^2\frac{1}{2m\sqrt{\rho}}\frac{\partial^2\sqrt{\rho}}{\partial x^2} \quad (5.13)$$

represents the Bohm quantum potential Bohm (1952).

Tunneling of a wave packet through a sequence of barriers effectively slows down the wavepacket spreading and the process becomes akin to quantum diffusion. Our numerical results can be simulated by adding a friction term, bv , on the left-hand side of the semiclassical equation (5.12), with b being a friction constant.

Inserting $\rho = \psi^*\psi$ for the wave packet, eq. (5.6), and allowing a time dependent width $\sigma(t)$, we obtain

$$m\frac{\partial^2\sigma}{\partial t^2} + b\frac{\partial\sigma}{\partial t} = \frac{\hbar^2}{4m\sigma^3} - \left\langle \frac{\partial V}{\partial x} \right\rangle, \quad (5.14)$$

where the last term contains an average with respect to the wavepacket. For a periodic potential and large values of σ , this term averages to zero ($\langle \partial V/\partial x \rangle = 0$) and $\sigma(t)$ can be obtained by solving the Eq. (5.14) for a general case, subject to the initial condition that $\sigma(t=0) = \sigma_0$.

There is a competition between the first and second derivatives on the left hand side of Eq. (5.14). One strategy to find the asymptotic time-dependence of $\sigma(t)$ is to solve Eq.

(5.14) neglecting one of the partial derivatives in different regimes and finding the value for which both solutions match. This procedure is validated by comparing to the numerical solutions of Eq. (5.14) for different set of values of m , b and σ_0 . The calculations show that after a transient time, and for a strongly bound molecule, the approximate result holds,

$$\sigma(t) \simeq 0.31 \left(\frac{\hbar^2 t}{mb\sigma_0^2} \right)^{1/2}, \quad (5.15)$$

where here m is the mass of the molecule. This asymptotic behavior is shown in figure (5.5).

Defining a diffusion coefficient by means of $D_d = \partial_t \sigma^2 / 2$, yields

$$D_d \sim 0.156 \frac{\hbar^2}{mb\sigma_0^2}. \quad (5.16)$$

Note the difference with the classical Einstein diffusion constant, $D_d = kT/b$. We argue that the effective “temperature” of this system is the kinetic energy of the initial state, $T \propto \hbar^2 / m\sigma_0^2$. The dependence of the temperature, or diffusion coefficient, on the initial kinetic energy is a new result to be tested experimentally. Notice, however, that these results might not hold when molecules interact among themselves.

For the dissociated molecules or atoms, the time-dependence of the spreading width of the atoms within the lattice is not well fitted by any power law dependence on time (dotted curve in figure 5.4). We observe a non-trivial correlation between $\sigma_{atoms}(t)$ and the molecule binding energy.

Currently, many of the optical lattice descriptions are based on the Bose-Hubbard Hamiltonian Jaksch et al. (1998), which is a tight-binding model. This Hamiltonian is familiar from strongly correlated systems and conveniently describes atom-atom interactions in many-atom systems. In addition, however, recent Feshbach resonance experiments in optical lattices call for the description of bound state molecule dynamics, including the diffusion by tunneling of atoms and molecules as well as the dissociation of molecules into atoms. In this work we have shown that the dissociation followed by tunneling of individual atoms gives rise to a complex dynamics, parts of which cannot be described by power law scaling at large times. This part requires additional theory follow-up. In our simple model

based on solving the time-dependent Schrödinger equation on a space-time lattice, we obtain fruitful insights into this dynamics. Some unexpected features such as the weakening of dissociation as the binding energies decreases, or the robustness of the molecule that tends to tunnel as a single compact object, are exhibited by the numerical results. We have also observed that the asymptotic time behavior of the spreading width of the molecules is amenable to an analytical treatment. A simple power law, $\sigma \propto t^{1/2}$, seems to arise from the numerical solutions. The diffusion of molecules and their dissociation during tunneling is a rich phenomenon which certainly deserves more research. The inclusion of interactions between the molecules, and atoms, in the dynamics of diffusion is also of great interest.

Appendix A

THE ONE-DIMENSIONAL WKB APPROXIMATION

Appendix A

We want to solve the Schrödinger equation for a particle:

$$\frac{\hbar^2}{2m} \frac{d^2}{dx^2} \psi(x) + [E - V(x)] \psi(x) = 0. \quad (\text{A.1})$$

For such, we will define a function σ and rewrite $\psi(x)$ as

$$\psi(x) = e^{i\sigma(x)/\hbar}. \quad (\text{A.2})$$

This leads to

$$\frac{1}{2m} \left(\frac{d}{dx} \sigma(x) \right)^2 - \frac{i\hbar}{2m} \frac{d^2}{dx^2} \sigma(x) = E - V(x). \quad (\text{A.3})$$

In a more compact notation we have

$$\sigma'^2 - i\hbar\sigma'' = 2m(E - V). \quad (\text{A.4})$$

The above equation reduces to the classical equation

$$\frac{1}{2m} \left(\frac{d}{dx} \sigma(x) \right)^2 = E - V(x).$$

in the limit $\hbar \rightarrow 0$. We expect that if quantum corrections are small (i.e. $\hbar \rightarrow 0$) then the solution of eq. (A.1) will be very close to the classical solution. The WKB approximation explores this fact¹.

Following the above argument we write σ in the form of a series of powers of \hbar :

$$\sigma = \sigma_0 + \frac{\hbar}{i} \sigma_1 + \left(\frac{\hbar}{i} \right)^2 \sigma_2 + \mathcal{O}(\hbar^3). \quad (\text{A.5})$$

Replacing this in eq. (A.4) and retaining the lowest powers of \hbar , we obtain

¹The acronym WKB is for Wentzel, Kramers and Brillouin.

$$\sigma_0'^2 + \frac{\hbar}{i}(2\sigma_1'\sigma_0' + \sigma_0'') + \left(\frac{\hbar}{i}\right)^2(\sigma_1'^2 + 2\sigma_2'\sigma_0' + \sigma_1'') + \mathcal{O}(\hbar^3) = 2m(E - V). \quad (\text{A.6})$$

Let us first neglect any term in eq. (A.6) that is proportional to any power of \hbar :

$$\sigma_0'^2 = 2m(E - V), \quad (\text{A.7})$$

which leads to

$$\sigma_0' = \pm\sqrt{2m(E - V)}.$$

We identify the term under the root as being the square of the classical momentum. Thus,

$$\sigma_0'(x) = \pm p(x), \quad (\text{A.8})$$

or

$$\sigma_0 = \pm \int p(x) dx \quad (\text{A.9})$$

This is the expression that we will use for σ_0 .

If the term in eq. (A.6) proportional to \hbar is negligible, the functions σ_0 and σ_1 should satisfy to the following condition:

$$2\sigma_1'\sigma_0' + \sigma_0'' \approx 0. \quad (\text{A.10})$$

That is,

$$\sigma_1' = -\frac{\sigma_0''}{2\sigma_0'} = -\frac{p'}{2p}, \quad (\text{A.11})$$

where we used eq. (A.8) and its derivative. Integrating this equation one obtains an expression for σ_1 :

$$\sigma_1 = -\frac{1}{2} \ln(p) = \ln(p^{-1/2}). \quad (\text{A.12})$$

Let us analyze, now, the term proportional to \hbar^2 . If we are going to neglect it, it should satisfy the following condition:

$$2\sigma'_0\sigma'_2 + \sigma_1'^2 + \sigma_1'' \approx 0. \quad (\text{A.13})$$

Using eq. (A.8), eq. (A.11), as well as the derivative of the latter one, we obtain the following expression for σ'_2 :

$$\sigma'_2 = \frac{p''}{4p^2} - \frac{2p'^2}{8p^3}. \quad (\text{A.14})$$

Integrating the first term by parts and introducing the force acting on the particle ($F = pp'/m$), we obtain a final expression for σ_2^2

$$\sigma_2 = \frac{1}{4}m\frac{F}{p^3} + \frac{1}{4}m^2 \int \frac{F^2}{p^5} dx. \quad (\text{A.15})$$

Conditions of validity

Given the values of σ_0 , σ_1 and σ_2 , we can determine an expression for the wave function and what conditions should be imposed so that it assumes a simple form. From eqs. (A.2) and (A.5), we obtain

$$\psi(x) = \exp\left(\frac{i}{\hbar}\sigma_0 + \sigma_1 + \frac{\hbar}{i}\sigma_2\right). \quad (\text{A.16})$$

With the use of the σ_i 's (eqs. (A.9), (A.12) and (A.15)), we obtain

$$\begin{aligned} \psi_{\pm} &= \frac{1}{\sqrt{p}} \exp\left(\pm \frac{i}{\hbar} \int p dx\right) \\ &\times \left[\exp\left(-i\hbar \frac{mF}{4p^3}\right) \exp\left(-i\hbar \frac{m^2}{4} \int \frac{F^2}{p^5}\right) \right], \end{aligned} \quad (\text{A.17})$$

²The expression of F is obtained starting from the derivative of eq. (A.8):

$$p' = \frac{d}{dx} \sqrt{2m(E-V)} = -\frac{m}{p} \frac{dV}{dx} = m \frac{F}{p}, \quad \text{i.e.,} \quad F = pp'/m.$$

where the terms inside the brackets are the contributions of σ_2 .

However, this expression is still very complicated. To simplify it, we will impose that the terms associated to σ_2 are negligible. This leads us to two conditions; the first is

$$\hbar m^2 \int \frac{F^2}{p^5} dx \ll 1. \quad (\text{A.18})$$

This condition is satisfied when F is small within distances of the order of λ , the particle's wavelength.

The second condition should be:

$$m\hbar \frac{F}{p^3} \ll 1. \quad (\text{A.19})$$

This condition can be rewritten in an alternative way. Recalling the relationship between F and p ($F = pp'/m$), eq. (A.19) becomes

$$\hbar \frac{p'}{p^2} \ll 1. \quad (\text{A.20})$$

That is the same as

$$\frac{d}{dx} \left(\frac{\hbar}{p} \right) \ll 1. \quad (\text{A.21})$$

As $\lambda = 2\pi\hbar/p$, we obtain

$$\frac{d}{dx} \left(\frac{\lambda}{2\pi} \right) \ll 1. \quad (\text{A.22})$$

This condition is of highest importance. A variation of λ should be small along distances of the order of one wave length.

Given these conditions (eqs. (A.18) and (A.22)), the wave function (eq. (A.17)) assumes the simplified expression

$$\psi_{\pm} = \frac{1}{\sqrt{p}} \exp \left[\pm \frac{i}{\hbar} \int p dx \right]. \quad (\text{A.23})$$

We have, here, two solutions that should be superimposed. Let us consider a situation as the one of the figure A.1.

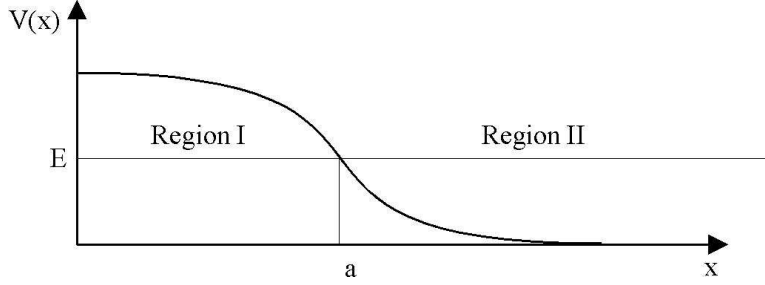


Figure A.1: Classically forbidden (I) and classically allowed (II) regions.

In the *classically allowed region* (region II), close to the turning point, $x = a$, the wave function should be a linear combination of ψ_+ and ψ_- :

$$\psi^{II} = \frac{C_1}{\sqrt{p}} \exp \left[\frac{i}{\hbar} \int_a^x p dx \right] + \frac{C_2}{\sqrt{p}} \exp \left[-\frac{i}{\hbar} \int_a^x p dx \right], \quad x > a. \quad (\text{A.24})$$

In the *classically forbidden region* (region I), to the left of $x = a$, we have a similar solution with two differences. The classical momentum p will be complex ($p = i|p|$) and, in order that ψ is quadratically integrable, C_2 should be zero. With that, the wave function in the classically forbidden region is:

$$\psi^I = \frac{C}{\sqrt{|p|}} \exp \left[\frac{1}{\hbar} \int_a^x |p| dx \right], \quad x < a. \quad (\text{A.25})$$

Notice that the above integral will always give a negative number, guaranteeing that the wave function is quadratically integrable.

Using the connection formulas discussed in the next section and combining eqs. (A.24), (A.33) and (A.35), we obtain the wave function in the classically allowed region:

$$\begin{aligned}
\psi^{II} &= \frac{C}{2\sqrt{k}} \exp \left[i \left(\int_a^x k(x) dx - \pi/4 \right) \right] \\
&\quad + \frac{C}{2\sqrt{k}} \exp \left[-i \left(\int_a^x k(x) dx - \pi/4 \right) \right], \quad x > a \\
&= \frac{C}{\sqrt{k}} \sin \left(\int_a^x k(x) dx + \pi/4 \right), \tag{A.26}
\end{aligned}$$

where $k(x) = p(x)/\hbar$. In the classically forbidden region, the wave function is:

$$\psi^I = \frac{C}{\sqrt{|k|}} \exp \left[\int_a^x |k(x)| dx \right], \quad x < a. \tag{A.27}$$

Connection formulas in WKB

We found above two wave functions, ψ^I and ψ^{II} . Neither of them is well defined in the proximity of the classical turning point $x = a$. In this region, the classical momentum tends to zero and the condition imposed by eq. (A.19) is not satisfied. In order to establish a continuity condition, we need to equalize ψ_I and ψ_{II} at a point different from a , for example at a point x' belonging to region I . This will only be possible if we can obtain the form of ψ_{II} in that region. However, on the real axis this task cannot be done, therefore it is only possible if we find a way to continue the wavefunction over a path not too close to a in passing from region II to region I . That is, we have to perform an analytic continuation of the wave function at the complex plane.

Let us consider a path which will bypass the point $x = a$. This path will be a semi-circle that will leave at point b , belonging to the region II , and arrive at the point x of the region I with a radius ρ . The order of magnitude of this radius should be large enough so that the conditions of validity of the WKB approximation are valid, but small enough so that we can expand $\sqrt{V(x) - E}$ as a Taylor series so that it converges quickly. This path can be made either at the upper semi-plane, or at the lower semi-plane and, in fact, we will do both.

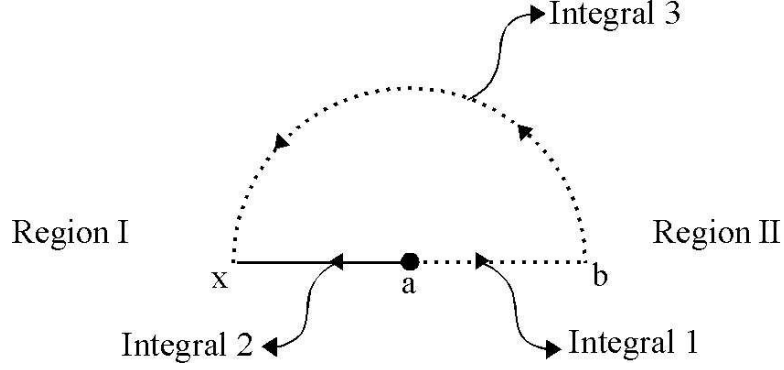


Figure A.2: Integration path in the complex plane for the connection formulas.

Given the condition on ρ discussed above, we can expand the function $V(x) - E$ in the following way:

$$\begin{aligned} V(x) - E &= V(a) - E + \frac{d(V(x) - E)}{dx}(x - a) + \mathcal{O}(x^2) \\ &= V(a) - E + \frac{dV(x)}{dx}(x - a) + \mathcal{O}(x^2). \end{aligned}$$

From the definition of a (turning point), $V(a) = E$. Identifying the derivative in the second term as the force upon the particle at the point a , we obtain

$$V(x) - E = F(a)(x - a) + \mathcal{O}(x^2) \approx F_0(x - a). \quad (\text{A.28})$$

With this, we obtain the following expressions for ψ^I and ψ^{II} along the complex path (from here up to eq. A.30, x will be taken as complex),

$$\begin{aligned} \psi^I(x) &= \frac{C}{(2m|F_0|(a-x))^{1/4}} \exp\left(\frac{1}{\hbar}\sqrt{2m|F_0|} \int_a^x \sqrt{a-x} dx\right), \quad x < a \\ \psi^{II}(x) &= \frac{C_1}{(2m|F_0|(x-a))^{1/4}} \exp\left(\frac{i}{\hbar}\sqrt{2m|F_0|} \int_a^x \sqrt{x-a} dx\right) \\ &\quad + \frac{C_2}{(2m|F_0|(x-a))^{1/4}} \exp\left(-\frac{i}{\hbar}\sqrt{2m|F_0|} \int_a^x \sqrt{x-a} dx\right), \quad \text{any } x. \end{aligned}$$

Now we define γ as $2m|F_0|$, and obtain:

$$\begin{aligned}\psi^I(x) &= \frac{C}{(\gamma(a-x))^{1/4}} \exp\left(\frac{1}{\hbar}\sqrt{\gamma} \int_a^x \sqrt{a-x} dx\right), \quad x < a \\ \psi^{II}(x) &= \frac{C_1}{(\gamma(x-a))^{1/4}} \exp\left(\frac{i}{\hbar}\sqrt{\gamma} \int_a^x \sqrt{x-a} dx\right) \\ &\quad + \frac{C_2}{(\gamma(x-a))^{1/4}} \exp\left(-\frac{i}{\hbar}\sqrt{\gamma} \int_a^x \sqrt{x-a} dx\right), \quad \text{any } x.\end{aligned}$$

As one bypasses the point $x = a$, one should determine the form that will assume the terms below the C 's as well as the integrands in the arguments of the exponentials in ψ^{II} . In both cases we have to find the function of $(x - a)$, that in the region II is larger than zero, but that in the region I is smaller than zero. This term always appears inside of a square root, so that it is interesting to maintain its sign explicitly.

In region I , as we by-pass the point $x = a$ on the upper semi-plane, we have:

$$(x - a) = -1(a - x) = e^{i\pi}(a - x), \quad (\text{A.29})$$

which leads to two substitutions in the wave function ψ^{II} :

$$\begin{aligned}\frac{1}{(x-a)^{1/4}} &= \frac{1}{(e^{i\pi}(a-x))^{1/4}} = \frac{e^{-i\pi/4}}{(a-x)^{1/4}}, \\ \int_a^x \sqrt{x-a} dx &= \int_a^x \sqrt{e^{i\pi}} \sqrt{a-x} dx \\ &= e^{i\pi/2} \int_a^x \sqrt{a-x} dx \\ &= i \int_a^x \sqrt{a-x} dx.\end{aligned} \quad (\text{A.30})$$

Using this result in ψ^{II} , we obtain:

$$\begin{aligned}\psi^{II}(x) &= \frac{C_1 e^{-i\pi/4}}{(\gamma(a-x))^{1/4}} \exp\left(\frac{i^2}{\hbar} \sqrt{\gamma} \int_a^x \sqrt{a-x} dx\right) \\ &+ \frac{C_2 e^{-i\pi/4}}{(\gamma(x-a))^{1/4}} \exp\left(-\frac{i^2}{\hbar} \sqrt{\gamma} \int_a^x \sqrt{a-x} dx\right).\end{aligned}$$

This can be rewritten as:

$$\begin{aligned}\psi^{II}(x) &= \frac{C_1}{(\gamma(a-x))^{1/4}} \exp\left(-\frac{1}{\hbar} \sqrt{\gamma} \int_a^x \sqrt{a-x} dx - i\frac{\pi}{4}\right) \\ &+ \frac{C_2}{(\gamma(x-a))^{1/4}} \exp\left(\frac{1}{\hbar} \sqrt{\gamma} \int_a^x \sqrt{a-x} dx - i\frac{\pi}{4}\right).\end{aligned}$$

Setting this equation equal to ψ^I we observe that all the denominators of the fractions are the same, and we thus obtain the following equation:

$$\begin{aligned}C_1 \exp\left(-\frac{1}{\hbar} \sqrt{\gamma} \int_a^x \sqrt{a-x} dx - i\frac{\pi}{4}\right) \\ + C_2 \exp\left(\frac{1}{\hbar} \sqrt{\gamma} \int_a^x \sqrt{a-x} dx - i\frac{\pi}{4}\right) \\ = C \exp\left(\frac{1}{\hbar} \sqrt{\gamma} \int_a^x \sqrt{a-x} dx\right).\end{aligned}\tag{A.31}$$

Now, as x goes away from a , the term that multiplies C_1 can be neglected before the other ones, leading to the following equation:

$$\begin{aligned}C_2 \exp\left(\frac{1}{\hbar} \sqrt{\gamma} \int_a^x \sqrt{a-x} dx - i\frac{\pi}{4}\right) \\ = C \exp\left(\frac{1}{\hbar} \sqrt{\gamma} \int_a^x \sqrt{a-x} dx\right),\end{aligned}\tag{A.32}$$

or

$$C_2 = C \exp\left(i\frac{\pi}{4}\right). \quad (\text{A.33})$$

Now it is necessary to determine C_1 . For this, we have to use an integration path along the inferior semi-plane and repeat all the steps we did above. It is straightforward to show that

$$\begin{aligned} C_1 \exp\left(\frac{1}{\hbar}\sqrt{\gamma} \int_a^x \sqrt{a-x} dx + i\frac{\pi}{4}\right) \\ = C \exp\left(\frac{1}{\hbar}\sqrt{\gamma} \int_a^x \sqrt{a-x} dx\right), \end{aligned} \quad (\text{A.34})$$

or

$$C_1 = C \exp\left(-i\frac{\pi}{4}\right). \quad (\text{A.35})$$

With this, we obtain C_2 and C_1 as a function of C . This explains eqs. (A.27) and (A.27).

Appendix B

SCHRÖDINGER EQUATION IN A SPACE-TIME LATTICE

Appendix B

For a small time step Δt between iterations, the time evolution of the Schrödinger equation can be written as

$$u(t + \Delta t, t) \simeq \frac{1 + (\Delta t/2i\hbar) H(t)}{1 - (\Delta t/2i\hbar) H(t)} u(t), \quad (\text{B.1})$$

where

$$H(t) = -\frac{\hbar^2}{2m} \frac{\partial^2}{\partial x^2} + V(x) + V_{int}(x, t)$$

is the Hamiltonian for a particle within a potential well $V(x)$ subject to an external potential $V_{int}(x, t)$. Eq. (B.1) is an implicit equation for the time evolution and is correct up to and including terms of the order $(\Delta t)^2$. It requires carrying out matrix multiplications and inversions at each iteration.

The operations $\mathcal{A} u$ in the r.h.s. of Eq. (B.1) is easy. The operation $\mathcal{A}^{-1} u$ is more complicated. The problem is to find the vector u in the equation

$$\mathbf{v} = \mathcal{A}^{-1} \mathbf{u}, \quad \text{where} \quad \mathbf{u} = \mathcal{A} \mathbf{v} \quad (\text{B.2})$$

\mathbf{u} is a vector composed with the $u^{(j)} = u(x_j, t)$ components of the wave-function $u(x, t)$. In Eq. (B.1) \mathcal{A} is a tri-diagonal operator (matrix). In matrix notation

$$\begin{pmatrix} v_1 \\ v_2 \\ \cdot \\ \cdot \\ \cdot \\ \cdot \\ v_N \end{pmatrix} = \begin{pmatrix} A_1 & 0 & 0 & \cdot & \cdot & 0 & \cdot \\ A_2^- & A_2 & A_2^+ & 0 & \cdot & \cdot & \cdot \\ 0 & A_3^- & A_3 & A_3^+ & 0 & \cdot & \cdot \\ \cdot & \cdot & \cdot & \cdot & \cdot & \cdot & \cdot \\ \cdot & \cdot & \cdot & \cdot & \cdot & \cdot & \cdot \\ 0 & \cdot & \cdot & \cdot & \cdot & \cdot & A_N \end{pmatrix} \begin{pmatrix} u_1 \\ u_2 \\ u_3 \\ \cdot \\ \cdot \\ \cdot \\ u_N \end{pmatrix}. \quad (\text{B.3})$$

This involves the following relations

$$A_i^- u_{i-1} + A_i u_i + A_i^+ u_{i+1} = v_i. \quad (\text{B.4})$$

Assuming a solution of the form

$$u_{i+1} = \alpha_i u_i + \beta_i \quad (\text{B.5})$$

and inserting in (B.4) we find the recursion relations for α_i and β_i :

$$\alpha_{i-1} = \gamma_i A_i^-, \quad \beta_{i-1} = \gamma_i (A_i^+ \beta_i - v_i) \quad (\text{B.6})$$

where

$$\gamma_i = -\frac{1}{A_i + \alpha_i A_i^+}. \quad (\text{B.7})$$

At the end of the lattice we assume $u_N = v_N$. This implies that $\alpha_{N-1} = 0$ and $\beta_{N-1} = v_N$.

For the problem defined by Eq. (B.1) we assume the second derivative to be given by $d^2 f(x)/dx^2 = [f(x_{j+1}) + f(x_{j-1}) - 2f(x_j)]/(\Delta x)^2$. Defining $\tau = \hbar \Delta t / 4m(\Delta x)^2$, Eq. (B.2) for the operation involving only the operator in denominator of Eq. (B.1) means that

$$A_k = \frac{1}{i\tau} + 2 + \frac{\Delta t}{2\hbar\tau} v_\alpha^{(k)}, \quad \text{and} \quad A_k^- = A_k^+ = -1. \quad (\text{B.8})$$

We can now determine α_i and β_i by running Eqs. (B.6) backwards from $i = N - 2$ down to $i = 1$. Then we use Eq. (B.5) running forward from $i = 2$ to N , assuming that u_1 at the other extreme of the lattice is given by $u_1 = v_1/A_1$.

Another way to solve the problem (B.3) for u is by a LU-decomposition, followed by a forward and backward substitution. This method does not need to involve the Dirichlet condition.

Let us assume that the A matrix in (B.3) can be written as a product of B and U matrix, where

$$A = LU = \begin{pmatrix} b_1 & c_1 & 0 & 0 & \dots \\ a_2 & b_2 & c_2 & 0 & \dots \\ 0 & a_3 & b_3 & c_3 & \dots \\ 0 & 0 & a_4 & b_4 & \dots \\ \dots & \dots & \dots & \dots & \dots \end{pmatrix} \quad (\text{B.9})$$

$$L = \begin{pmatrix} 1 & 0 & 0 & 0 & \dots \\ \alpha_2 & 1 & 0 & 0 & \dots \\ 0 & \alpha_3 & 1 & 0 & \dots \\ 0 & 0 & \alpha_4 & 1 & \dots \\ \dots & \dots & \dots & \dots & \dots \\ \dots & \dots & \dots & \dots & \dots \end{pmatrix} \quad U = \begin{pmatrix} \beta_1 & \alpha_1 & 0 & 0 & \dots \\ 0 & \beta_2 & \gamma_2 & 0 & \dots \\ 0 & 0 & \beta_3 & \gamma_3 & \dots \\ 0 & 0 & 0 & \beta_4 & \dots \\ \dots & \dots & \dots & \dots & \dots \\ \dots & \dots & \dots & \dots & \dots \end{pmatrix}. \quad (\text{B.10})$$

Then, $Au = v \rightarrow L(Uu) = v$, or $Ly = v$. The elements of y are

$$\begin{pmatrix} y_1 \\ y_2 \\ y_3 \\ y_4 \\ \dots \\ \dots \\ \dots \\ y_N \end{pmatrix} = \begin{pmatrix} \beta_1 & \gamma_1 & 0 & 0 & \dots \\ 0 & \beta_2 & \gamma_2 & 0 & \dots \\ 0 & 0 & \beta_3 & \gamma_3 & \dots \\ 0 & 0 & 0 & \beta_4 & \dots \\ 0 & 0 & \dots & \dots & \dots \end{pmatrix} \begin{pmatrix} u_1 \\ u_2 \\ u_3 \\ u_4 \\ \dots \\ \dots \\ \dots \\ u_N \end{pmatrix}. \quad (\text{B.11})$$

This can be solved by backwards substitution

$$u_N = \frac{y_N}{\beta_N}, \quad \beta_i u_i + \gamma_i u_{i+1} = y_i, \quad (\text{B.12})$$

or

$$u_i = (y_i - \gamma_i u_{i+1}) / \beta_i. \quad (\text{B.13})$$

The other matrix equation

$$\begin{pmatrix} 1 & 0 & 0 & 0 & \cdot & \cdot \\ \alpha_2 & 1 & 0 & 0 & \cdot & \cdot \\ 0 & \alpha_3 & 1 & 0 & \cdot & \cdot \\ 0 & 0 & \alpha_4 & 1 & \cdot & \cdot \\ \cdot & \cdot & \cdot & \cdot & \cdot & \cdot \end{pmatrix} \begin{pmatrix} y_1 \\ y_2 \\ y_3 \\ y_4 \\ \cdot \\ \cdot \\ \cdot \\ y_N \end{pmatrix} = \begin{pmatrix} v_1 \\ v_2 \\ v_3 \\ v_4 \\ \cdot \\ \cdot \\ \cdot \\ v_N \end{pmatrix} \quad (\text{B.14})$$

can be solved by forward substitution

$$y_1 = v_1, \quad \alpha_i y_{i-1} + y_i = v_i, \quad (\text{B.15})$$

or

$$y_i = v_i - \alpha_i y_{i-1}. \quad ((\text{D.15}))$$

Now, we need to find α_i and β_i as a function of the original elements of \mathcal{A}

$$\begin{pmatrix} 1 & 0 & 0 & 0 & \cdot & \cdot & \cdot \\ \alpha_2 & 1 & 0 & 0 & \cdot & \cdot & \cdot \\ 0 & \alpha_3 & 1 & 0 & \cdot & \cdot & \cdot \\ 0 & 0 & \alpha_4 & 1 & \cdot & \cdot & \cdot \\ \cdot & \cdot & \cdot & \cdot & \cdot & \cdot & \cdot \\ \cdot & \cdot & \cdot & \cdot & \cdot & \cdot & \cdot \end{pmatrix} \begin{pmatrix} \beta_1 & \gamma_1 & 0 & 0 & \cdot & \cdot & \cdot \\ 0 & \beta_2 & \gamma_2 & 0 & \cdot & \cdot & \cdot \\ 0 & 0 & \beta_3 & \gamma_3 & \cdot & \cdot & \cdot \\ 0 & 0 & 0 & \beta_4 & \cdot & \cdot & \cdot \\ \cdot & \cdot & \cdot & \cdot & \cdot & \cdot & \cdot \\ \cdot & \cdot & \cdot & \cdot & \cdot & \cdot & \beta_N \end{pmatrix} \\ = \begin{pmatrix} b_1 & c_1 & 0 & 0 & \cdot & \cdot & \cdot \\ a_2 & b_2 & c_2 & 0 & \cdot & \cdot & \cdot \\ 0 & a_3 & b_3 & c_3 & \cdot & \cdot & \cdot \\ 0 & 0 & a_4 & b_4 & \cdot & \cdot & \cdot \\ \cdot & \cdot & \cdot & \cdot & \cdot & \cdot & \cdot \\ \cdot & \cdot & \cdot & \cdot & \cdot & \cdot & \cdot \end{pmatrix}$$

which implies

$$b_1 = \beta_1, \quad b_2 = \alpha_2 \gamma_1 + \beta_2, \quad \dots, \quad b_i = \gamma_{i-1} \alpha_i + \beta_i.$$

or

$$\beta_i = b_i - \gamma_{i-1} \alpha_i, \quad c_i = \gamma_i. \quad (\text{B.16})$$

Also,

$$a_2 = \beta_1 \alpha_2, \quad a_3 = \beta_2 \alpha_3, \quad \dots, \quad a_i = \beta_{i-1} \alpha_i,$$

or

$$\alpha_i = \frac{a_i}{\beta_{i-1}}. \quad (\text{B.17})$$

Thus, knowing a_i , b_i and c_i , one can go upwards with this set of equations to solve the problem.

In our particular case,

$$a_i = c_i = -1. \quad (\text{B.18})$$

Thus, the above equations simplify to

$$\begin{aligned} \beta_1 &= b_1, & \beta_i &= b_i - \frac{1}{\beta_{i-1}}, & i &= 2, \dots, N \\ y_1 &= v_1, & y_i &= v_i + \frac{y_{i-1}}{\beta_{i-1}}, & i &= 2, \dots, N \\ u_N &= \frac{y_N}{\beta_N}, & u_i &= \frac{(y_i + u_{i+1})}{\beta_i}, & i &= N-1, \dots, 1. \end{aligned} \quad (\text{B.19})$$

These operations completely solve the problem in Eq. (B.1) to find $u(t + \Delta t)$ in terms of $u(t)$. The extension to higher-dimensions is done by using a sequence of operations such as in Eq. (B.1) for each coordinate. In other words,

$$\begin{aligned} u(t + \Delta t, t) &\simeq U_x(t) U_y(t) \cdots u(t) \\ &= \left[\frac{1 + (\Delta t / 6i\hbar) H_x(t)}{1 - (\Delta t / 6i\hbar) H_x(t)} \right] \left[\frac{1 + (\Delta t / 6i\hbar) H_y(t)}{1 - (\Delta t / 6i\hbar) H_y(t)} \right] \cdots u(t), \end{aligned} \quad (\text{B.20})$$

where the first bracket and the notation H_x means that only the propagation along the direction x is done in the lattice, keeping the function values unchanged along the other coordinates. To improve numerical convergence, the x, y, \dots operations can be swapped and the results averaged for each time step.

Bibliography

- Arimondo, E., & Wimberger, S. (2011). Tunneling of ultracold atoms in time-independent potentials. *arXiv*, *1104.2535*, 1–25.
- Bailey, T., Bertulani, C., & Timmermans, E. (2010). Quantum diffusion in optical lattices. In *APS Meeting Abstracts*, (p. 1003P).
- Ben Dahan, M., Peik, E., Reichel, J., Castin, Y., & Salomon, C. (1996). Bloch oscillations of atoms in an optical potential. *Physical Review Letters*, *76*(24), 4508–4511.
- Bertulani, C. A. (2011). Fusion11 conference summary. *arXiv*, *1105.6356*, 1–10.
- Bertulani, C. A., Flambaum, V. V., & Zelevinsky, V. G. (2007). Tunneling of a composite particle: effects of intrinsic structure. *Journal of Physics G: Nuclear and Particle Physics*, *34*(11), 2289–2295.
- Bloch, I., & Zwerger, W. (2008). Many-body physics with ultracold gases. *Reviews of Modern Physics*, *80*(3), 885–964.
- Bohm, D. (1952). A suggested interpretation of the quantum theory in terms of "hidden" variables. i. *Physical Review*, *85*(2), 166–179.
- Brink, A. M., Odintsov, A. A., Bobbert, P. A., & Schön, G. (1991). Coherent cooper pair tunneling in systems of josephson junctions: Effects of quasiparticle tunneling and of the electromagnetic environment. *Zeitschrift für Physik B Condensed Matter*, *85*(3), 459–467.
- Chin, C., Julienne, P., & Tiesinga, E. (2010). Feshbach resonances in ultracold gases. *Reviews of Modern Physics*, *82*(2), 1225–1286.
- Donley, E. A., Claussen, N. R., Cornish, S. L., Roberts, J. L., Cornell, E. A., & Wieman, C. E. (2001). Dynamics of collapsing and exploding bose-einstein condensates. *Nature*, *412*, 295–299.

- Feshbach, H. (1958). Unified theory of nuclear reactions*. *Annals of Physics*, 5(4), 357–390.
- Görlitz, A., Vogels, J. M., Leanhardt, A. E., Raman, C., Gustavson, T. L., Abo-Shaeer, J. R., Chikkatur, A. P., Gupta, S., Inouye, S., Rosenband, T., & Ketterle, W. (2001). Realization of bose-einstein condensates in lower dimensions. *Physical Review Letters*, 87(13), 130402.
- Greiner, M., & Fölling, S. (2008). Condensed-matter physics: Optical lattices. *Nature*, 453(7196), 736–738.
- Jaksch, D., Bruder, C., Cirac, J. I., Gardiner, C. W., & Zoller, P. (1998). Cold bosonic atoms in optical lattices. *Physical Review Letters*, 81(15), 3108–3111.
- Klumpp, A., Witthaut, D., & Korsch, H. J. (2007). Quantum transport and localization in biased periodic structures under bi- and polychromatic driving. *Journal of Physics A: Mathematical and Theoretical*, 40(10), 2299–2311.
- Korsch, H. J., & Mossmann, S. (2003). An algebraic solution of driven single band tight binding dynamics. *Physics Letters A*, 317, 54–63.
- Krems, R. V., Stwalley, W. C., & Friedrich, B. (Eds.) (2009). *Cold molecules: theory, experiment, applications*. Boca Raton, FL: CRC Press.
- Landau, L. D., & Lifshits, E. M. (1958). *Quantum mechanics, non-relativistic theory*, vol. v.3 of *Their Course of theoretical physics*. London: Pergamon Press.
- Lewenstein, M., & Liu, W. V. (2011). Optical lattices: Orbital dance. *Nature*, 7, 101–103.
- Orso, G., Pitaevskii, L. P., Stringari, S., & Wouters, M. (2005). Formation of molecules near a feshbach resonance in a 1d optical lattice. *Physical Review Letters*, 95(6), 060402.
- Press, W. H., Teukolsky, S. A., Vetterling, W. T., & Flannery, B. P. (2007). *Numerical Recipes: The Art of Scientific Computing*. New York, NY: Cambridge University Press, 3rd ed.
- Sachdev, S. (2008). Quantum magnetism and criticality. *Nature Physics*, 4(3), 173.

- Thalhammer, G., Winkler, K., Lang, F., Schmid, S., Grimm, R., & Denschlag, J. H. (2006). Long-lived feshbach molecules in a three-dimensional optical lattice. *Physical Review Letters*, *96*(5), 050402.
- Tsuchiya, S., & Ohashi, Y. (2008). Anomalous enhancement of quasiparticle current near a potential barrier in a bose-einstein condensate. *Physical Review A*, *78*(1), 013628.
- Varga, R. S. (1962). *Matrix iterative analysis*. Englewood Cliffs, NJ: Prentice-Hall.
- Wouters, M., & Orso, G. (2006). Two-body problem in periodic potentials. *Physical Review A*, *73*(1), 012707.
- Zhong, J., Diener, R. B., Steck, D. A., Oskay, W. H., Raizen, M. G., Plummer, E. W., Zhang, Z., & Niu, Q. (2001). Shape of the quantum diffusion front. *Physical Review Letters*, *86*(12), 2485–2489.

VITA

Taylor Chase Bailey, the youngest son of Wesley and Vicky Bailey, was born in Roxton, Texas, on May 24, 1986. Taylor attended Roxton Independent School District, during which time he spent an interim year at Barton Saint Peter's Church of England Primary School. He went on to confer his diploma from Roxton High School in 2004. He has earned an Associate of Science from Paris Junior College and went on to receive his Bachelor's of Science from Texas A&M University-Commerce in Physics and Mathematics in 2009. He then proceeded to obtain his Master's of Science in Physics from Texas A&M University-Commerce.

